

University of Alabama in Huntsville

**LOUIS**

---

Theses

UAH Electronic Theses and Dissertations

---

2008

## Study of the stability of scaled uncontrolled kinetic energy kill projectiles

Serena Osborne

Follow this and additional works at: <https://louis.uah.edu/uah-theses>

---

### Recommended Citation

Osborne, Serena, "Study of the stability of scaled uncontrolled kinetic energy kill projectiles" (2008).  
*Theses*. 423.  
<https://louis.uah.edu/uah-theses/423>

This Thesis is brought to you for free and open access by the UAH Electronic Theses and Dissertations at LOUIS. It has been accepted for inclusion in Theses by an authorized administrator of LOUIS.

**STUDY OF THE STABILITY OF SCALED UNCONTROLLED KINETIC  
ENERGY KILL PROJECTILES**

**by**

**SERENA OSBORNE**

**A THESIS**

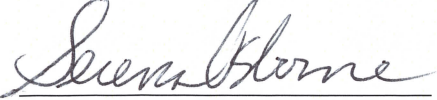
**Submitted in partial fulfillment of the requirements  
for the degree of Master of Science in Engineering  
in  
The Department of Mechanical and Aerospace Engineering  
to  
The School of Graduate Studies  
of  
The University of Alabama in Huntsville**

**HUNTSVILLE, ALABAMA**

**2008**



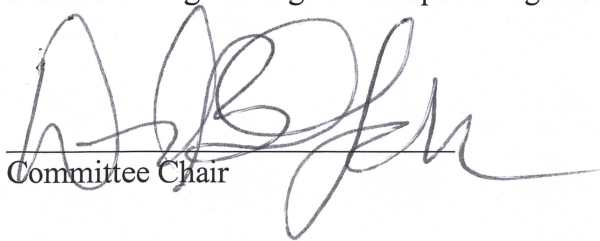
In presenting this thesis in partial fulfillment of the requirements for a master's degree from The University of Alabama in Huntsville, I agree that the Library of this University shall make it freely available for inspection. I further agree that permission for extensive copying for scholarly purposes may be granted by my advisor or, in his/her absence, by the Chair of the Department or the Dean of the School of Graduate Studies. It is also understood that due recognition shall be given to me and to The University of Alabama in Huntsville in any scholarly use which may be made of any material in this thesis.

      3/13/08  
(student signature)                      (date)

## THESIS APPROVAL FORM

Submitted by Serena Osborne in partial fulfillment of the requirements for the degree of Master of Science in Engineering in Aerospace Engineering and accepted on behalf of the faculty of the School of Graduate Studies by the thesis committee.

We, the undersigned members of the graduate faculty of the University of Alabama in Huntsville, certify that we have advised and/or supervised the candidate on the work described in this thesis. We further certify that we have reviewed the thesis manuscript and approve it in partial fulfillment of the requirements for the degree of Master of Science in Engineering in Aerospace Engineering.

  
Committee Chair

3/11/08  
Date

H.W. Coleman  
Committee

3/11/08  
Date

Robert A. Fredrick  
Committee

3/11/08  
Date

Kader Fouda  
Department Chair

3/12/08  
Date

J.P. C  
College Dean

3/13/08  
Date

William M. Mowbray  
Graduate Dean

4/30/08  
Date

## ABSTRACT

The School of Graduate Studies  
The University of Alabama in Huntsville

Degree: Master of Science in Engineering

College/Dept: Engineering/Mechanical  
and Aerospace Engineering

Name of Candidate: Serena G. Osborne

Title: Study of the Stability of Scaled Uncontrolled Kinetic Energy Kill Projectiles

Hypervelocity impact testing is an important aspect of lethality assessment of tactical kinetic energy weapons. Ballistic ranges are often used for this purpose. It was observed that light gas gun ballistic projectile tests in the University of Alabama in Huntsville Aerophysics Research Center (UAH ARC) produce unacceptably large impact angles ( $> 2^\circ$ ) in a helium test gas. However impact angles below this limit were consistently observed when nitrogen was used. The goal of the research presented in this thesis was to determine if the Projectile Design and Analysis System (PRODAS) could be used to design a projectile that will meet the yaw and pitch limits. Because PRODAS only simulates an air atmosphere, a simple pressure scaling method was developed to calculate an equivalent air pressure with the density and temperature of the helium test gas. The Response Surface Method (RSM) was used with the pressure scaled PRODAS code to design a projectile that met the impact angle requirements. The resultant projectile design was fabricated and flown demonstrating acceptable impact angles.

Abstract Approval:

  
Committee Chair

3/11/08  
Date

  
Department Chair

3/12/08  
Date

  
Graduate Dean

4/30/08  
Date

## **ACKNOWLEDGMENTS**

I would like to thank Dr. Brian Landrum for his advisement in my coursework and this thesis. I would like to thank Dr. Robert Frederick for making PRODAS accessible for this research. The PRODAS code was provided under an academic agreement with Arrow Tech Associates. I appreciate the support from Tim Carroll in using DigSim and analyzing data. I would like to thank the UAH ARC, especially Brian Akins, for providing his knowledge about the range and for allowing me to perform an actual test for this project. I appreciate the support given to me by my employer, KBM Enterprises Inc., while completing this thesis. I would also like to thank my husband for supporting me in this process.

# TABLE OF CONTENTS

	Page
LIST OF FIGURES .....	ii
LIST OF TABLES .....	v
CHAPTER	
ONE INTRODUCTION .....	1
1.1 <i>Ballistics Range Applications</i> .....	1
1.2 <i>Model Stability Analysis</i> .....	2
TWO DESIGN TOOLS .....	5
2.1 <i>PRODAS Overview</i> .....	5
2.2 <i>Geometric Modeling</i> .....	7
2.3 <i>Mass Properties</i> .....	9
2.4 <i>Aerodynamics and Stability Evaluation</i> .....	10
2.5 <i>Trajectory Simulation</i> .....	13
2.6 <i>DigSim 6-DoF</i> .....	14
2.7 <i>Response Surface Method</i> .....	18
THREE PRODAS CALIBRATION PROCESS .....	24
3.1 <i>PRODAS and DigSim Comparison</i> .....	24
3.2 <i>Predicting the LGG Test using DigSim</i> .....	30
3.3 <i>Predicting LGG Test using PRODAS</i> .....	35
3.4 <i>Predicting Pitch and Yaw Limit in PRODAS</i> .....	44



FOUR	OPTIMUM PROJECTILE DESIGN.....	46
	4.1 <i>Projectile Design Matrix</i> .....	46
	4.2 <i>PRODAS/RSM Run Matrix Results</i> .....	48
	4.3 <i>RSM Analysis</i> .....	49
FIVE	ARC LGG TEST .....	54
	5.1 <i>ARC 133 LGG</i> .....	54
	5.2 <i>0744 Test Geometry</i> .....	56
	5.3 <i>0744 LGG Test and Results</i> .....	58
	5.4 <i>0744 PRODAS Model</i> .....	61
	5.5 <i>0744 PRODAS Trajectory Analysis</i> .....	63
SIX	SUMMARY AND CONCLUSIONS .....	65
	APPENDIX: DigSim SAMPLE INPUT FILE .....	69
	REFERENCES .....	72

## LIST OF FIGURES

Figure	Page
2.1 PRODAS Common Data Structure [2] .....	6
2.2 Baseline 0430 ARC Projectile Geometry (dimensions in inches) and Machined Projectile .....	6
2.3 PRODAS Model Editor Screen for the Baseline Projectile Geometry [6] .....	8
2.4 PRODAS Flare Element [6].....	9
2.5 PRODAS Mass Properties Screen for the Baseline Projectile [6].....	10
2.6 PRODAS Aerodynamics Model of the Baseline Projectile [6] .....	11
2.7 PRODAS Stability Evaluation and MET Data Screens for FINNER Aerodynamics of the Baseline Projectile [6].....	12
2.8 PRODAS 6-DoF Initial Conditions Screen [6].....	13
2.9 PRODAS 6-DoF Example Baseline Projectile Pitch Plot [6].....	14
2.10 Block Diagram of DigSim 6-DoF .....	15
2.11 Baseline Projectile Normal Force Slope Comparison .....	17
2.12 Baseline Projectile Center of Pressure Comparison .....	17
2.13 Baseline Projectile Axial Force Comparison.....	18
2.14 Baseline Projectile Damping Derivative Comparison .....	18
2.15 Face Centered Cube Design (FCD) [5].....	21
3.1 Baseline Projectile Yaw vs. Time Predicted by DigSim and PRODAS.....	25
3.2 Baseline Projectile Pitch vs. Time Predicted by DigSim and PRODAS .....	26
3.3 Baseline Projectile Velocity vs. Time Predicted by DigSim and PRODAS.....	26
3.4 Baseline Projectile X-distance vs. Time Predicted by DigSim and PRODAS .....	27

3.5 Baseline Projectile Yaw vs. Time Predicted by Modified DigSim and PRODAS.....	28
3.6 Baseline Projectile Pitch vs. Time Predicted by Modified DigSim and PRODAS ....	28
3.7 Baseline Projectile Velocity vs. Time Predicted by Modified DigSim and PRODAS	29
3.8 Baseline Projectile X-distance vs. Time Predicted by Modified DigSim and PRODAS.....	29
3.9 Break Screen Before and After 0430 LGG test .....	31
3.10 X-ray Image of Pitch for ARC 0430 LGG Test.....	31
3.11 X-ray Image of Yaw for ARC 0430 LGG Test .....	32
3.12 Impact Point Before and After 0430 LGG Test.....	32
3.13 Baseline Projectile Yaw vs. Time Predicted by DigSim .....	33
3.14 Baseline Projectile Pitch vs. Time Predicted by DigSim.....	34
3.15 Baseline Projectile Velocity vs. Time Predicted by DigSim .....	34
3.16 Baseline Projectile X-distance vs. Time Predicted by DigSim.....	35
3.17 PRODAS Stability Evaluation Screen for M-Fr Mid-body Scaled Model [6] .....	38
3.18 PRODAS Stability Evaluation Screen for M-Fr Diameter Scaled Model [6] .....	39
3.19 Yaw vs. Time for Simulated Helium in PRODAS .....	41
3.20 Pitch vs. Time for Simulated Helium in PRODAS.....	42
3.21 X-distance vs. Time for Simulated Helium in PRODAS .....	42
3.22 Yaw vs. Time for Air and Simulated Helium in PRODAS .....	43
3.23 Pitch vs. Time for Air and Simulated Helium in PRODAS .....	44
4.1 2 <sup>nd</sup> -Order RSM Coefficients for Pitch and Yaw .....	51
4.2 RSM Residuals for Pitch and Yaw .....	53
5.1 133 mm ARC LGG Pump and Launch Tube.....	54



5.2 133 mm ARC LGG Impact Chamber .....	55
5.3 UAH ARC 133 mm LGG Range Schematic .....	55
5.4 0744 ARC projectile (Dimensions in inches) .....	57
5.5 0744 ARC Machined Projectile .....	58
5.6 Break Screen Before and After 0744 LGG Test.....	59
5.7 Pitch for ARC 0744 LGG Test .....	60
5.8 Yaw for ARC 0744 LGG Test .....	60
5.9 Impact Point Before and After 0744 LGG Test.....	61
5.10 PRODAS Aerodynamics Model of 0744 Projectile [6].....	62
5.11 PRODAS Stability Evaluation Screen for 0744 Projectile [6] .....	62
5.12 0744 PRODAS Predicted Pitch vs. Time for two Pitch Tip-off Rates .....	64
5.13 0744 PRODAS Predicted Yaw vs. Time for two Yaw Tip-off Rates .....	64

## LIST OF TABLES

Table	Page
2.1 FCD Matrix for Three Coded Variables .....	22
2.2 Matrix of Independent Variables for $2^3$ Factorial Design.....	23
3.1 Modified Equation of State Property Data.....	40
3.2 Baseline Projectile Simulation Attitude and Distance Comparison .....	43
4.1 Range of Independent Projectile Design Variables .....	47
4.2 PRODAS RSM Run Matrix.....	47
4.3 PRODAS Coded RSM Run Matrix .....	48
4.4 PRODAS RSM Run Matrix Results.....	49
4.5 PRODAS vs. RSM Attitudes .....	52
5.1 133 mm LGG Dimensions .....	55
5.2 Geometry Modifications .....	57

## CHAPTER ONE

### INTRODUCTION

#### *1.1 Ballistics Range Applications*

An increased need for high fidelity simulations of an entire missile system has been established by the defense community. The University of Alabama in Huntsville Aerophysics Research Center (UAH ARC) ballistic range has been launching scaled projectiles to facilitate missile research and development since its inception. The ballistic range provides a relatively low cost, fast turnaround test as compared to expensive full-scale flight tests. The capability to test a scaled model of a missile system early in the design process allows for validation of theoretical codes that predict system performance, as well as identifying flaws in the concept before full-scale testing and production begin [1].

One major ballistic range application is the study of hypervelocity impact phenomena. This includes experiments to support the evaluation of kinetic energy weapons for tactical systems and kill assessment. Types of hypervelocity impact tests include single or multiple rods and fragments and numerous configurations of hit-to-kill projectiles. The range also provides the capability to vary projectile mass and materials.

From these tests the ARC enables evaluation of important parameters such as strike angle, strike velocity, and pitch and yaw attitude [1].

### *1.2 Model Stability Analysis*

Several weapon systems currently being developed rely on kinetic energy kill mechanisms. For such a system to be effective, the projectile's pitch and yaw angles relative to the target must be close to zero. Model stability has been historically problematic with the Light Gas Gun (LGG) at the ARC ballistic range. This is mainly due to the projectile flying in a closed environment with dirt, debris, and little time or space for correction. The ARC uses helium or nitrogen gases in the LGG instead of air. These gases inhibit fires in the flight range when the hydrogen driver gas exits the muzzle. They also help cool and slow the muzzle blast better than air, and thus minimize blast effects on fragile targets. When using helium, the sonic speed is approximately 3 times faster than air, reducing the projectile's Mach number considerably. This minimizes the drag between the muzzle and projectile. Gun efficiency is also reduced when using air because a more dense gas has to be pushed out of the barrel ahead of the model. This wastes energy that could be used to accelerate the projectile.

It was observed that the LGG helium tests did not meet the maximum  $2^\circ$  requirement for pitch and yaw impact angle. However this limit was consistently met when nitrogen was used. Active controls to help stabilize the projectile are not possible in the LGG. This is due to a flight time (approximately 21 milliseconds) too short for a control response. Therefore, changing the model's geometry (flare angle, cone angle, and

body length) and/or environment to try and meet the pitch/yaw attitude limits is necessary.

To predict a scaled projectile's stability, it is common practice to use analysis tools to simulate the flight of a candidate configuration including geometry and environment. After much research, it was decided the best high fidelity tool available for trajectory modeling and stability analysis of projectiles was the Projectile Design and Analysis System (PRODAS) by ARROW TECH Associates [2]. PRODAS combines a user defined geometric model along with user inputs to analyze physical properties, exterior and interior ballistics, structure, and terminal ballistics of a projectile. It also has the capability to analyze 4-DoF and 6-DoF flight trajectories [3]. The software's modular architecture simplifies projectile analysis through high level analysis algorithms, a shared database, and user friendly interface [2].

The goal of the research presented in this thesis was to determine if PRODAS can be used to predict projectile configurations that will meet the maximum  $2^\circ$  limit for pitch and yaw attitude in ARC LGG helium tests. The first step was to compare existing ARC LGG projectile test data shot in helium with PRODAS predictions. This posed a problem because PRODAS only simulates an air atmosphere. Therefore, a method to simulate helium in PRODAS had to be developed. In order to make sure this method was appropriate, a stand-alone 6-DoF called DigSim [4], capable of running in any environment (air, helium, nitrogen, etc.), was used as a baseline. First, PRODAS 6-DoF predictions for the baseline projectile and air atmosphere were compared with DigSim



predictions for the same projectile and atmosphere to see what, if any, differences existed. A methodology for using PRODAS with a scaled air atmosphere was developed to mimic flight in helium. DigSim predictions for the baseline projectile in helium were used to verify the PRODAS predictions for simulated helium. The PRODAS code with simulated helium was then used to design a modified projectile to meet the  $2^\circ$  maximum limit for pitch and yaw attitude. Last, a matrix of projectile configurations consisting of various nose cone angles, mid-body lengths, and tail flare angles was developed and run in PRODAS with simulated helium to determine which would meet the  $2^\circ$  limit for pitch and yaw impact attitude.

The Response Surface Methodology (RSM) [5] was used to aid in the projectile configuration analysis. RSM represents a statistical technique to improve or optimize processes and develop new ones. RSM is most widely used in industry where performance or quality of a product is influenced by several variables. This same approach can be applied to the pitch/yaw attitude analysis of the ARC projectiles.

Using the predictions obtained from PRODAS and RSM, a projectile design was obtained that met the attitude limits. This model design was fabricated and tested in the 133 mm LGG. The actual LGG test day conditions and model geometry were then simulated by PRODAS and predictions were compared back to the test data.

## **CHAPTER TWO**

### **DESIGN TOOLS**

#### *2.1 PRODAS Overview*

The Projectile Design and Analysis System (PRODAS) software by ARROW TECH Associates [3] uses a geometric model along with user inputs to analyze physical properties, ballistics (interior, exterior, and terminal), and structures of projectiles. PRODAS was developed using proven methodologies and techniques, most of which are based on experimental testing. A diagram of the PRODAS analysis options is shown in Figure 2.1. Using a common database, PRODAS has the capability to feed the results of one analysis directly into another subsequent analysis providing continuity. For example, stability analysis results are passed to the trajectory analysis to evaluate projectile motion. The flexibility of the PRODAS modular architecture allows its capabilities to be continually updated as new and improved simulated methods evolve [2].

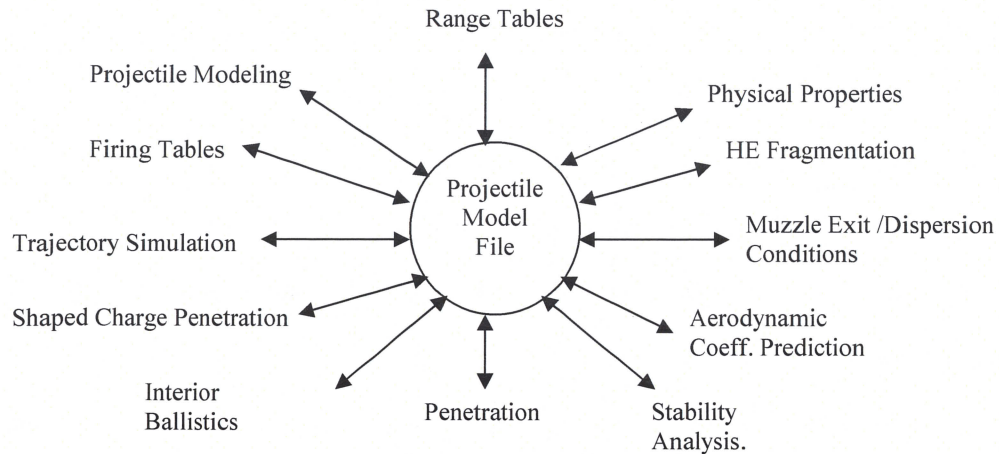


Figure 2.1 PRODAS Common Data Structure [2]

A baseline ARC projectile was used to demonstrate the capabilities of PRODAS.

Figure 2.2 shows the 0430 baseline geometry and machined projectile. It consists of a long rod made of carbon steel with an epoxy sleeve and a  $15^\circ$  half-angle cone shaped nose and a  $45^\circ$  half-angle flare tail made of aluminum. The projectile mass is 71.8 grams with a CG of 110.06 mm (4.33 in) from the nose. It has a body diameter of 12.7 mm (0.5 in) and a tail diameter of 27.94 mm (1.1 in).

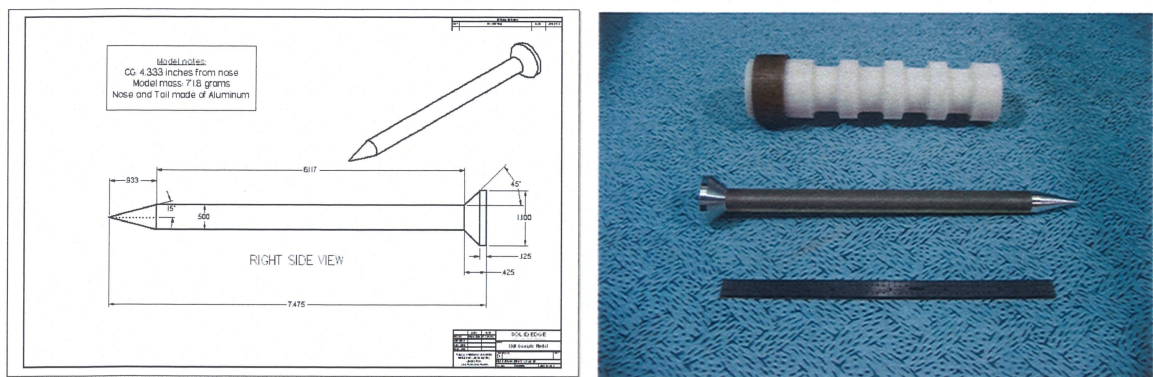


Figure 2.2 Baseline 0430 ARC Projectile Geometry (dimensions in inches) and Machined Projectile



## 2.2 Geometric Modeling

The first step with PRODAS is to define a geometric model of the projectile. This model is used as input by all other analysis options inside PRODAS. The basic units of a model are called elements. Elements can be frustums or symmetric fins and must have an aerodynamic function (*wetted, ogive, fin, flare, etc.*). Components (*body, band, nose, windscreen, etc.*) are used to define the material properties and physical descriptions of a collection of elements. Assemblies consist of a collection of components or other assemblies.

The PRODAS *Model Editor* can be used to build the geometric model from scratch or one can be imported from a computer-aided design (CAD) system. Due to the simplicity of the projectile geometry in this study, the *Model Editor* was used to build the baseline model. The result is shown in Figure 2.3. The first step is to name a component and then define its material properties. This can be done manually or by using the *Materials Reference Book* inside PRODAS. Next, a physical function is assigned to describe the primary purpose of the component and if it is consumable or not. Examples of physical functions are *structural, drag stabilized, penetrator, sabot, band, HE, tracer, and liner*.

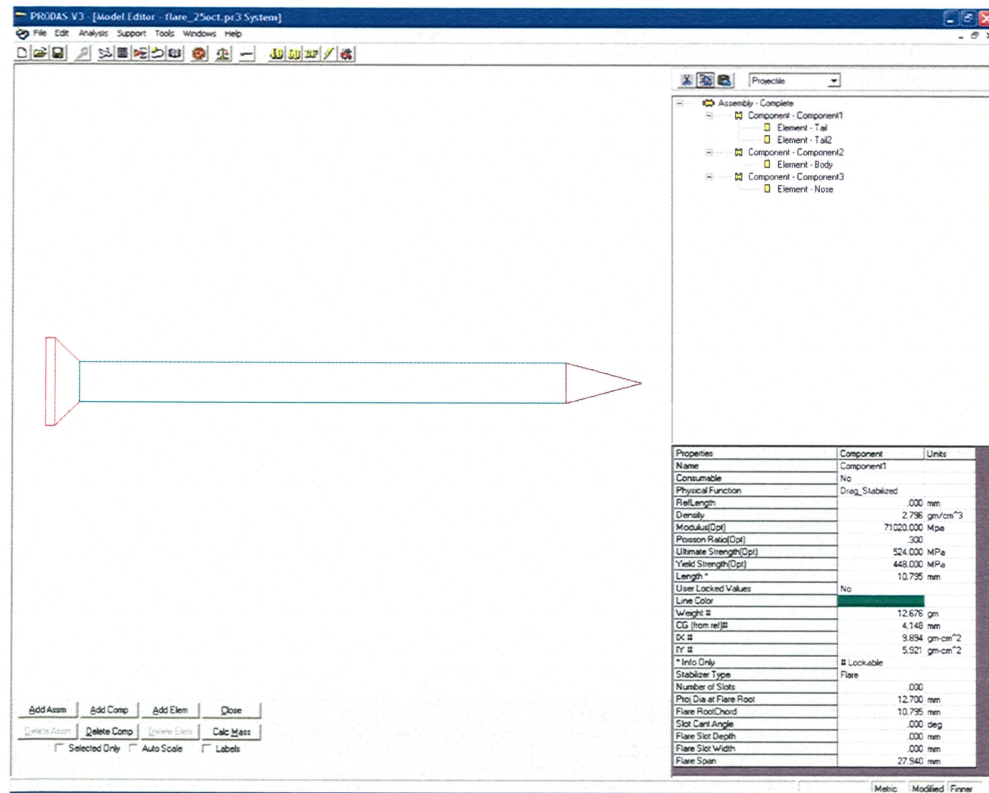


Figure 2.3 PRODAS Model Editor Screen for the Baseline Projectile Geometry [6]

The next step is to define the elements that make up each component. Each element in a component must have the same material properties. All elements excluding fins are axisymmetric about the longitudinal axis. Figure 2.4 shows the flare element of the baseline projectile tail component. Each element is described by 8 parameters: *Left Diameter*, *Right Diameter*, *Element Length*, *Reference Distance*, *Aerodynamic Function*, *Void*, *Geometric Type*, and *Radius*. The diameter values are input and the void is specified by yes or no. The void option allows for more complex elements such as hollow ones to be built. Lastly, the aerodynamic function is defined. It is very important to select the correct function due to the aerodynamic calculations being performed. Options for aerodynamic function include *wetted*, *ogive*, *band*, *none*, *fin*, *flare*, *grove*, *boom*, *boattail*, and *spike*.

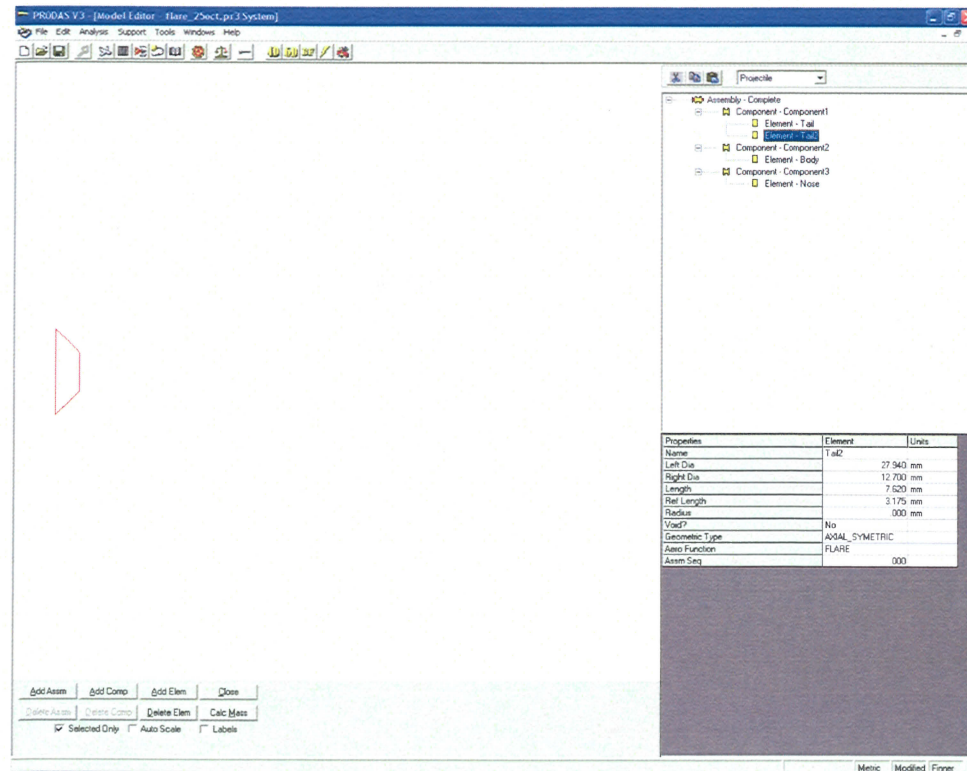


Figure 2.4 PRODAS Flare Element [6]

### 2.3 Mass Properties

Once the projectile geometry is defined, its mass properties can be calculated by selecting *Mass Properties* from the analysis menu. This module calculates weights, inertias, and CG based on the model inputs. The mass is calculated from the component volumes and densities. Axisymmetric elements, which make up the baseline projectile, are computed by summing frustums. The *Mass Properties* window for the baseline projectile is shown in Figure 2.5. Because PRODAS doesn't have material properties for carbon steel and epoxy, aluminum was chosen to make up the mid-body. For PRODAS to better approximate the mass of the 0430 projectile, an approximate aluminum (aluminum with a density change) was used for the mid-body.



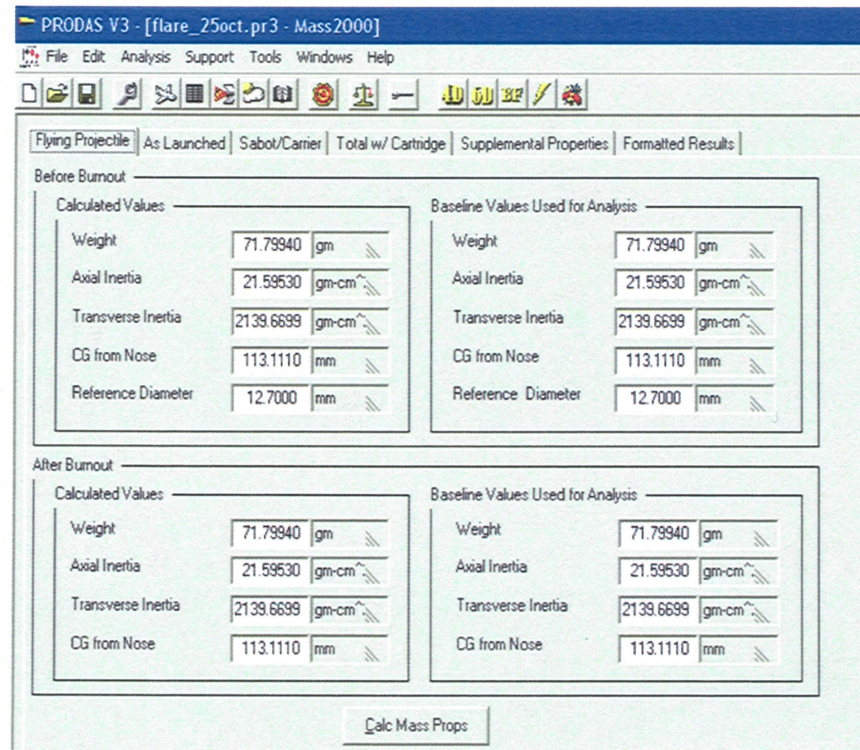


Figure 2.5 PRODAS Mass Properties Screen for the Baseline Projectile [6]

## 2.4 Aerodynamics and Stability Evaluation

Calculating the projectile aerodynamic coefficients is the next step. PRODAS uses internal SPINNER [7] and FINNER [8] codes to do this. These are empirical codes based on analysis of free flight, wind tunnel, and test range data for several hundred projectiles. Body alone coefficients are computed by the SPINNER code while the fin and flare coefficients are computed by the FINNER code. The SPINNER code predicts axial force and pitching moment coefficients to within  $\pm 3\%$  and normal force coefficients to within  $\pm 4\%$ . The FINNER code predicts these coefficients to within  $\pm 7\%$ . Both codes are continually updated as new data becomes available to expand their range and capability of predicting projectile aerodynamic coefficients [7, 8].

Aerodynamic predictions are run by selecting *Aerodynamics* under the PRODAS analysis menu. The screen that opens is helpful in checking the input data before calculating the new aero coefficients. A simplified model is created by PRODAS using the user input projectile geometry. Figure 2.6 shows the 0430 baseline ARC projectile (top) compared to the PRODAS model (bottom). The two models are very similar in key features such as overall length and nose cone length and radius. However, the flat end on the flare is not modeled in the PRODAS aerodynamic coefficient calculation. This causes the PRODAS model flare angle to be approximately  $35^\circ$  versus the  $45^\circ$  angle of the real geometry. This affected the aerodynamics as discussed in Sections 2.6 and 3.1. Using the PRODAS aerodynamics ultimately resulted in lower tip-off rates to predict the 0430 baseline test.

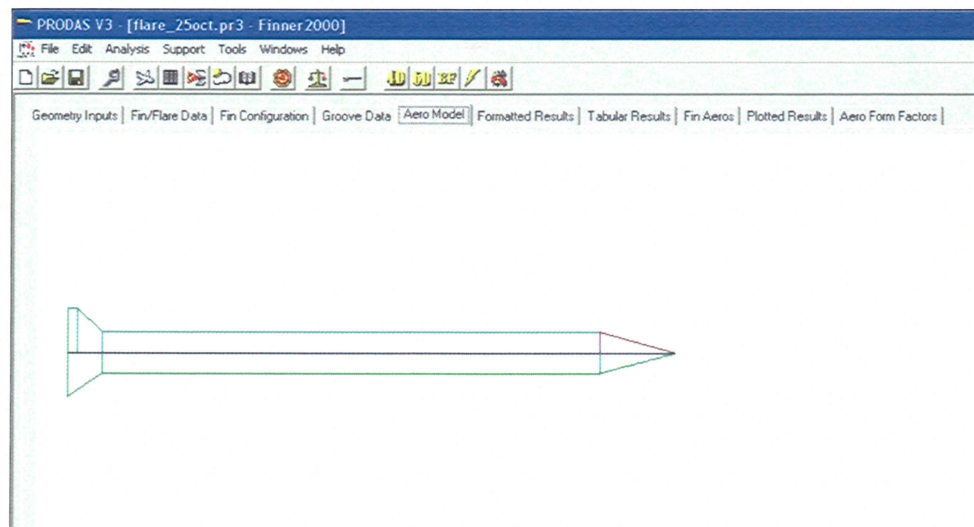


Figure 2.6 PRODAS Aerodynamics Model of the Baseline Projectile [6]



An initial estimate of the model stability is obtained by selecting *Stability Evaluation* under the *Aerodynamics* tab. This module uses SPINNER aerodynamics if the projectile is spin stabilized and FINNER aerodynamics if it has fins or a flare. Since the baseline projectile is flare stabilized, the FINNER aerodynamic model is used.

Figure 2.7 shows the *Stability Evaluation* screen. This screen gives details such as muzzle velocity, center of pressure (CP), center of gravity (CG), static margin, and gyroscopic stability factor ( $S_{go}$ ). For flared projectiles the CP should be aft of the CG for the model to be stable. Another indication of stability for a flared projectile is the static margin. This is the distance between the CP and CG. The desired value is at least 0.5 calibers.  $S_{go}$  is only calculated for Spinner models.

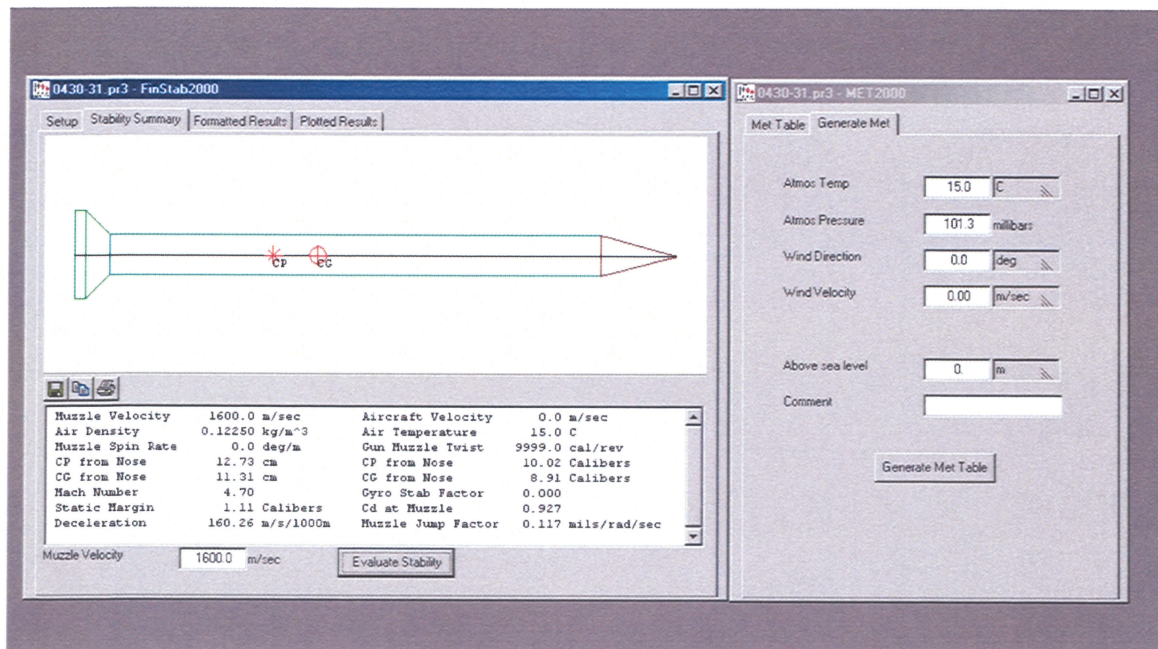


Figure 2.7 PRODAS Stability Evaluation and MET Data Screens for FINNER Aerodynamics of the Baseline Projectile [6]

Figure 2.7 also shows the *MET* atmospheric data screen. The *MET* option gives the user the ability to change the temperature, pressure, and wind characteristics of air for the analysis.

## 2.5 Trajectory Simulation

Many other options exist under the PRODAS analysis menu, but this thesis concentrates on the *Trajectory* analysis using the 6 Degree-of-Freedom (6-DoF) option. This option allows the user to simulate a projectile's trajectory given its initial conditions such as gun elevation and azimuth, muzzle velocity, spin, twist, and starting position. The results are available in tabular or plot format. Figure 2.8 shows an example of the 6-DoF trajectory initial conditions input screen. Figure 2.9 is an example output plot of pitch versus time for the baseline projectile. Pitch is positive nose up and Yaw is positive nose right.

Aero Form Factors		Formatted Results		Tabular Results		Plotted Results	
Setup/Run		Output Setup		Initial Conditions		Projectile Parameters	
<b>Gun Setup</b>							
Quadrant Elevation	1.000	deg					
Gun Azimuth	0.000	deg					
Met Table Source	User						
<b>Projectile Initial Position</b>							
Initial X position	0.	m					
Initial Y position	0.	m					
Initial Z position	0.	m					
Start at Time	0.000	sec					
<b>Projectile Spin Rate</b>							
Muzzle Velocity	1610.0	m/sec					
Spin at Muzzle	0.	rad/sec					
Twist	9999.00	cal/rev					
Exit Spin Ratio	0.00						
Calculate Spin							
<b>Projectile Angles and Rates</b>							
Initial Pitch Angle	0.0	deg					
Initial Yaw Angle	0.0	deg					
Initial Pitch Rate	679.0	deg/sec					
Initial Yaw Rate	289.3	deg/sec					

Figure 2.8 PRODAS 6-DoF Initial Conditions Screen [6]



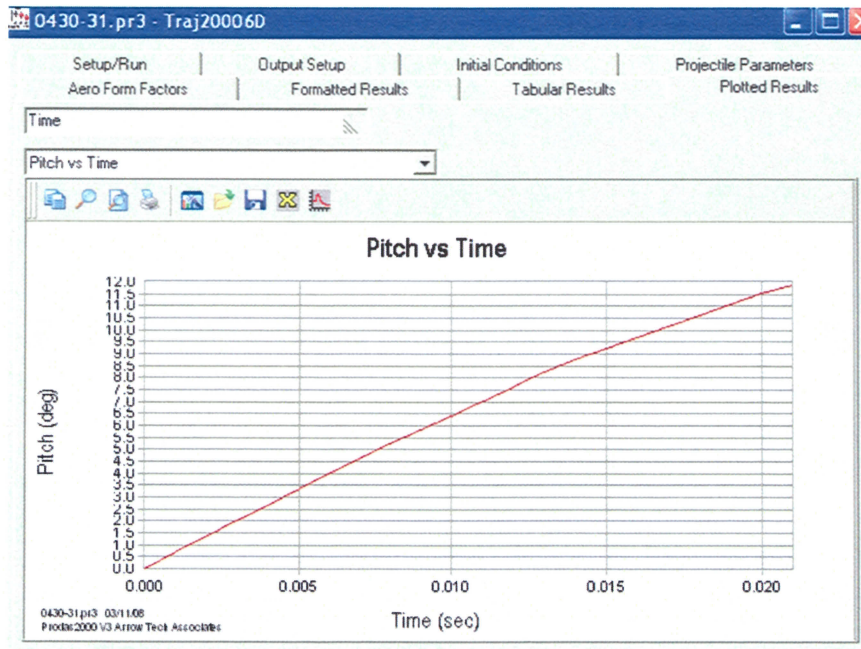


Figure 2.9 PRODAS 6-DoF Example Baseline Projectile Pitch Plot [6]

## 2.6 DigSim 6-DoF

DigSim is a 6-DoF simulation driver developed by Van Brewer of Nichols Research Corporation for the System Simulation and Development Directorate, US Army Missile Command. It provides the user a simply structured basic framework that is flexible, extensible, and adaptable [4]. DigSim has been used on many Army missile programs including FOG-M, TOW, CKEM, Boar, MSTAR, Hydra-70, JTUAV, and MLRS-TGSM. The validity of this simulation has been established by numerous comparisons with flight test data.

DigSim is written in FORTRAN that consists of two parts. The first part is called the *simulation executive*, and the second part is the *simulation models*. The *simulation executive* is a discrete event asynchronous simulation driver that handles input and output, numerical integration, incrementing time, and calling the simulation models. A



discrete event happens at a specific point in time. No discrete events were required for the simulations in this thesis. Asynchronous operation is where the simulation maintains a list of events and their corresponding execution times [4]. A fourth order Runge-Kutta numerical integration technique was used for this analysis.

A pictorial representation of the DigSim 6-DoF is shown in Figure 2.10. This contains all of the modules necessary to model the projectile's flight through a particular medium such as equations of motion and force and moment calculations. It uses the WGS 84 compliant oblate spheroid earth model [9]. This earth model handles the geometry, Coriolis acceleration, centripetal acceleration, earth's rotation rate and gravity. The atmosphere model was modified for constant property inputs of pressure, temperature, gas constant ( $R$ ), and ratio of specific heats ( $\gamma$ ). The outputs of the atmospheric model are density and speed of sound. The outputs of the

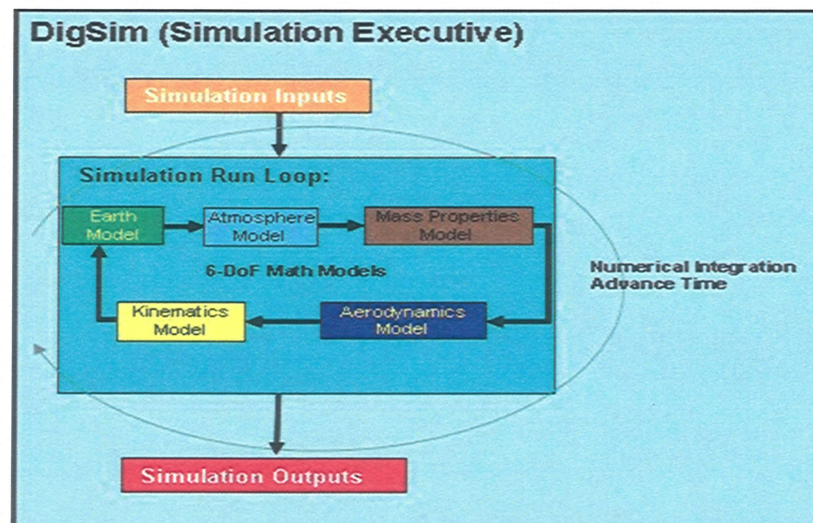


Figure 2.10 Block Diagram of DigSim 6-DoF

The mass properties model simply contains constants for the mass, center of gravity, and inertias for the projectile. The mass properties calculated from PRODAS were used as input to be consistent. The aerodynamic model calculates the aerodynamic forces and moments acting on the projectile. The kinematics model contains the equations of motion for 3 translational degrees of freedom and 3 rotational degrees of freedom. A quaternion method is used to propagate the projectiles attitude.

The aerodynamic model is based on data from DATCOM [10]. A comparison of the aerodynamic coefficients between DATCOM and PRODAS (FINNER) for the baseline projectile is shown in Figures 2.11 through 2.14. The primary differences are for low supersonic ( $M < 1.5$ ) and subsonic aerodynamic predictions. One reason the aerodynamics are different is due to PRODAS not modeling the flat end on the flare which DATCOM does model. Another reason is due to different aerodynamic prediction methodologies. DATCOM is primarily a theory based predictive method with some empirical methods focused on missile configurations. The PRODAS FINNER code is primarily an empirically based predictive method with some theoretical methods focused on bullets and projectiles. To provide consistent comparisons of the baseline projectile aerodynamics between PRODAS and DigSim, the aerodynamic coefficients calculated by PRODAS were used in DigSim.

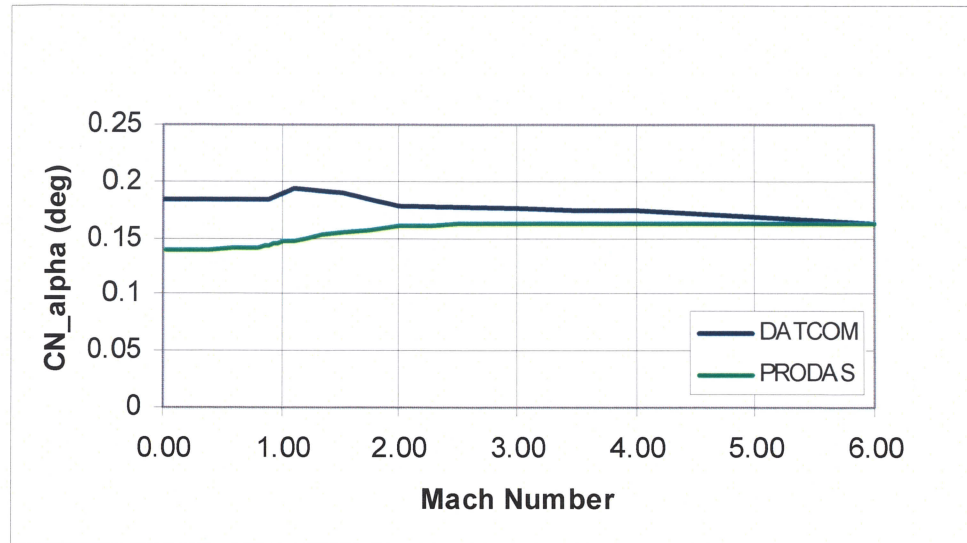


Figure 2.11 Baseline Projectile Normal Force Slope Comparison

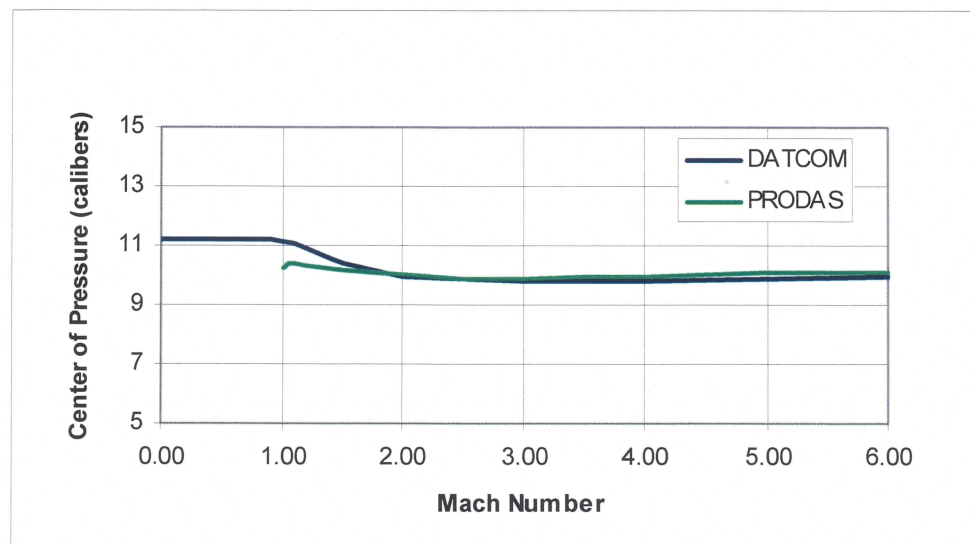


Figure 2.12 Baseline Projectile Center of Pressure Comparison



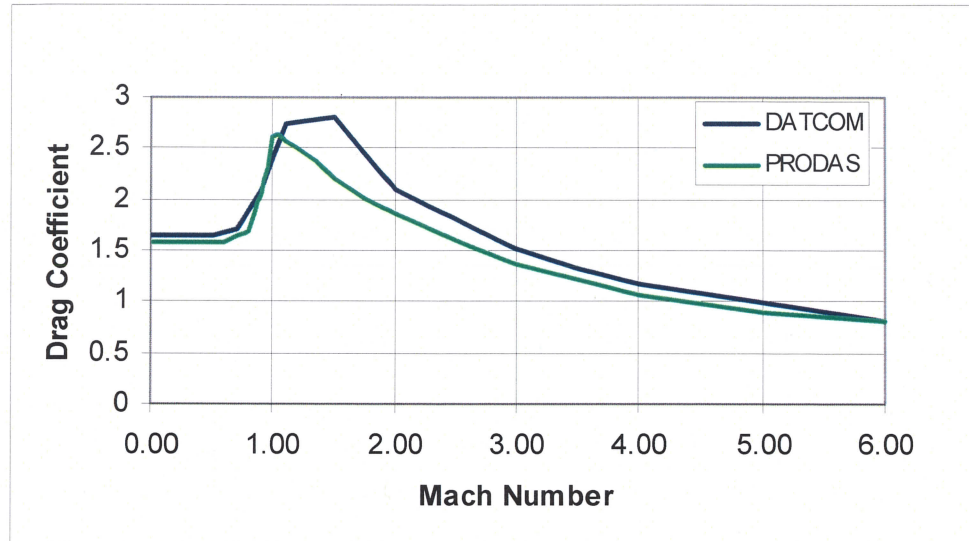


Figure 2.13 Baseline Projectile Axial Force Comparison

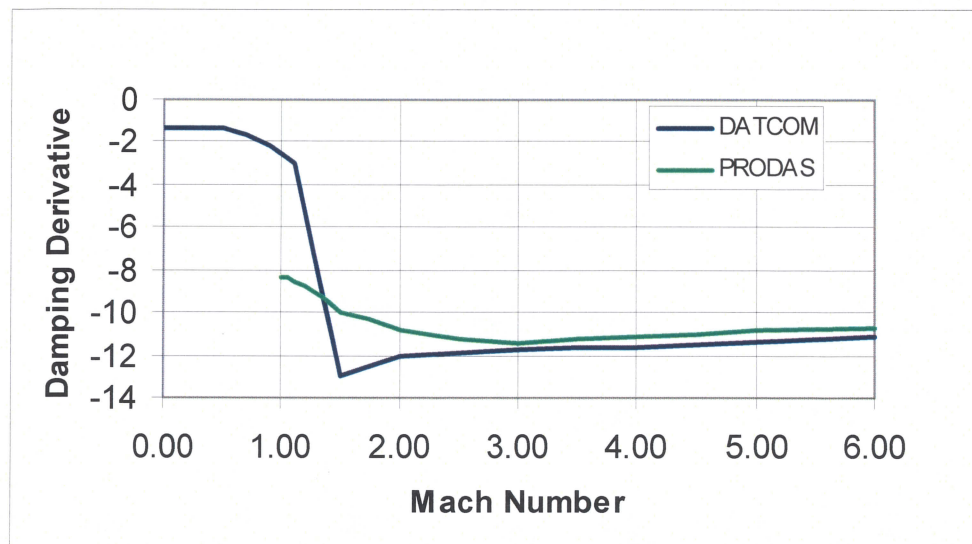


Figure 2.14 Baseline Projectile Damping Derivative Comparison

## 2.7 Response Surface Method

The Response Surface Method (RSM) uses statistical techniques to help improve or optimize processes and develop new ones. It is useful in designing and developing new products and improving existing designs. RSM is most widely used in industry

where performance or quality of a product is influenced by several variables [5]. This performance measure is known as the *response* and the input variables are called *independent variables*. The inputs are defined by the analyst depending on the purpose of the analysis. For this study, the *input variables* are the body length, tail flare and nose angles, and the *response* is the pitch/yaw attitude of the projectile.

The RSM success is highly dependent on the estimate of the true response function. In most cases a first-order or second-order model is used. A first-order model is usually good enough if one is interested in approximating the response for a small region of the independent variable space where little curvature exists. Most often a second-order model is used due to the fact that it can take on many functional forms, and its parameters are easily estimated [5]. An example of a first-order response is given by

$$y = \beta_0 + \beta_1 X_1 + \beta_2 X_2 + \beta_3 X_3 + \beta_{12} X_1 X_2 + \beta_{23} X_2 X_3 + \beta_{13} X_1 X_3 + \beta_{123} X_1 X_2 X_3, \quad (2.1)$$

where  $y$  is the *response*,  $\beta_j$  are the *regression coefficients*, and  $X_k$  are the *regression variables*. The parameters  $\beta_j$  are the change in response  $y$  per unit change in each  $x_j$  holding all other independent variables constant [5].

Nonlinear influences are taken into account when using the second-order response equation

$$y = \beta_0 + \beta_1 X_1 + \beta_2 X_2 + \beta_3 X_3 + \beta_{12} X_1 X_2 + \beta_{23} X_2 X_3 + \beta_{13} X_1 X_3 + \beta_{11} X_1^2 + \beta_{22} X_2^2 + \beta_{33} X_3^2 + \beta_{123} X_1 X_2 X_3 \quad (2.2)$$

This can be rewritten to look linear in its parameters to yield the equation

$$y = \beta_0 + \beta_1 X_1 + \beta_2 X_2 + \beta_3 X_3 + \beta_{12} X_1 X_2 + \beta_{23} X_2 X_3 + \beta_{13} X_1 X_3 + \beta_4 x_4 + \beta_5 X_5 + \beta_6 X_6 + \beta_{123} X_1 X_2 X_3 \quad (2.3)$$

Therefore, this is called a linear regression model regardless of the shape of the response it generates [5].

There are several ways to estimate the  $\beta$ -coefficients in a linear regression model.

The most common method is the least squares method. The  $\beta$  values are chosen so that the sum of the squares of the errors is at a minimum. Thus, the least squares estimator of  $\beta$  is given by

$$\mathbf{b} = (\mathbf{X}'\mathbf{X})^{-1} \mathbf{X}'\mathbf{y} , \quad (2.4)$$

where  $\mathbf{b}$  is the vector of least squares estimators,  $\mathbf{X}$  is a matrix of *independent variables*,  $\mathbf{X}'$  is the transpose of  $\mathbf{X}$ , and  $\mathbf{y}$  is the *response*. The diagonal terms of matrix  $\mathbf{X}'\mathbf{X}$  represent the sums of squares, and the off-diagonal terms are the sums of the cross-products of the elements in  $\mathbf{X}$ . The fitted model is given by

$$\hat{\mathbf{y}} = \mathbf{X}\mathbf{b} . \quad (2.5)$$

The residual, given by

$$\mathbf{e} = \mathbf{y} - \hat{\mathbf{y}} , \quad (2.6)$$

is the difference between the actual response,  $y_i$ , and the fitted value  $\hat{y}_i$  [5].

There are many experimental designs for fitting second-order models. The central composite design (CCD) is most widely used. Strict ranges are applied to design variables so that the region of interest and operability are the same. That is, the specified ranges for the independent design variables should produce a result near the optimum. For a design consisting of 3 independent variables and 2 levels of interest (high/low), the result is a cube, as shown in Figure 2.15, and the area of interest is on the inside and perimeter of the cube. This is known as a  $2^3$  factorial design. It is most often called the face-centered cube design (FCD) because the axial points occur at the centers of the faces rather than outside the faces [5].

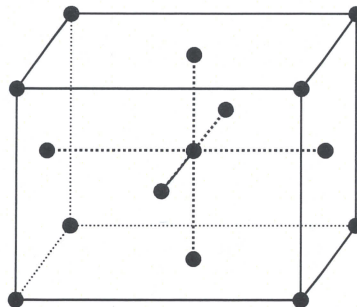


Figure 2.15 Face Centered Cube Design (FCD) [5]



The FCD requires one simulation run for each point on the cube or 15 total simulation runs. Because the independent variables can have different units and ranges, coded values are defined to produce dimensionless analysis. The coded values range from +1 for the high value to -1 for the low value so that they affect the response,  $y$ , more evenly. The coded variable values are determined from the physical values by

$$X_i = 2 \left( \frac{X - X_{avg}}{X_{range}} \right), \quad (2.7)$$

where  $X_i$  is the coded value,  $X$  is the independent variable,  $X_{avg}$  is the average of the maximum and minimum independent variable, and  $X_{range}$  is the difference in the maximum and minimum independent variable. Table 2.1 shows the FCD matrix for the coded (normalized) variables.

Table 2.1 FCD Matrix for Three Coded Variables

Run	$X_1$	$X_2$	$X_3$
1	-1	-1	-1
2	1	-1	-1
3	-1	1	-1
4	1	1	-1
5	-1	-1	1
6	1	-1	1
7	-1	1	1
8	1	1	1
9	1	0	0
10	-1	0	0
11	0	1	0
12	0	-1	0
13	0	0	1
14	0	0	-1
15	0	0	0



Table 2.2 was developed using the coded variables from Table 2.1. It represents the matrix of independent variables,  $\mathbf{X}$ , from equation 2.4, used to determine the vector of least squares estimators,  $\mathbf{b}$ . Column 1 represents an identity element. Columns 2 through 4 represent the main effects variables ( $X_1$ ,  $X_2$ ,  $X_3$ ) shown in Table 2.1, and columns 5 through 11 represent the interaction between the main effects variables.

Table 2.2 Matrix of Independent Variables for  $2^3$  Factorial Design

I	$X_1$	$X_2$	$X_3$	$X_1X_2$	$X_1X_3$	$X_2X_3$	$X_1X_2X_3$	$X_1^2$	$X_2^2$	$X_3^2$
1	-1	-1	-1	1	1	1	-1	1	1	1
1	1	-1	-1	-1	-1	1	1	1	1	1
1	-1	1	-1	-1	1	-1	1	1	1	1
1	1	1	-1	1	-1	-1	-1	1	1	1
1	-1	-1	1	1	-1	-1	1	1	1	1
1	1	-1	1	-1	1	-1	-1	1	1	1
1	-1	1	1	-1	-1	1	-1	1	1	1
1	1	1	1	1	1	1	1	1	1	1
1	1	0	0	0	0	0	0	1	0	0
1	-1	0	0	0	0	0	0	1	0	0
1	0	1	0	0	0	0	0	0	1	0
1	0	-1	0	0	0	0	0	0	1	0
1	0	0	1	0	0	0	0	0	0	1
1	0	0	-1	0	0	0	0	0	0	1
1	0	0	0	0	0	0	0	0	0	0

RSM was used in this thesis study to determine which of the geometric parameters (flare angle, body length, or cone angle) of the baseline projectile most affected the pitch and yaw attitude of the trajectory. RSM aided in the selection of the best projectile geometry to shoot at the ARC that would meet the maximum  $2^\circ$  limit for pitch and yaw attitude.

## CHAPTER THREE

### PRODAS CALIBRATION PROCESS

#### *3.1 PRODAS and DigSim Comparison*

Because PRODAS does not have the capability to model helium in its 6-DoF trajectory simulation, a direct comparison to the ARC LGG data could not be made. Therefore a similarity analysis was performed to derive a method for scaling PRODAS to model helium. The DigSim 6-DoF simulation has the capability to model helium and was used to calibrate PRODAS.

The first step in the calibration process was to compare the two simulations using air. The baseline projectile trajectory was calculated by PRODAS and DigSim at the same conditions of an atmospheric pressure of 13.32 kPa, temperature of 300K, velocity of 1610 m/s, and tip-off rates of 9 rad/s along with the same mass properties and aerodynamic coefficients. Initially DigSim used the aerodynamics for the baseline projectile determined with DATCOM. As discussed in Chapter 2, the aerodynamics from DigSim are slightly different due to DATCOM modeling the flat end of the flare where PRODAS does not. Comparisons between the two simulations using different aerodynamics are shown in Figures 3.1 through 3.4. The yaw and pitch angles differ by

as much as 0.5 degrees through out the flight time, the velocity differs by as much as 0.6 m/s and X position predictions are in very close agreement.

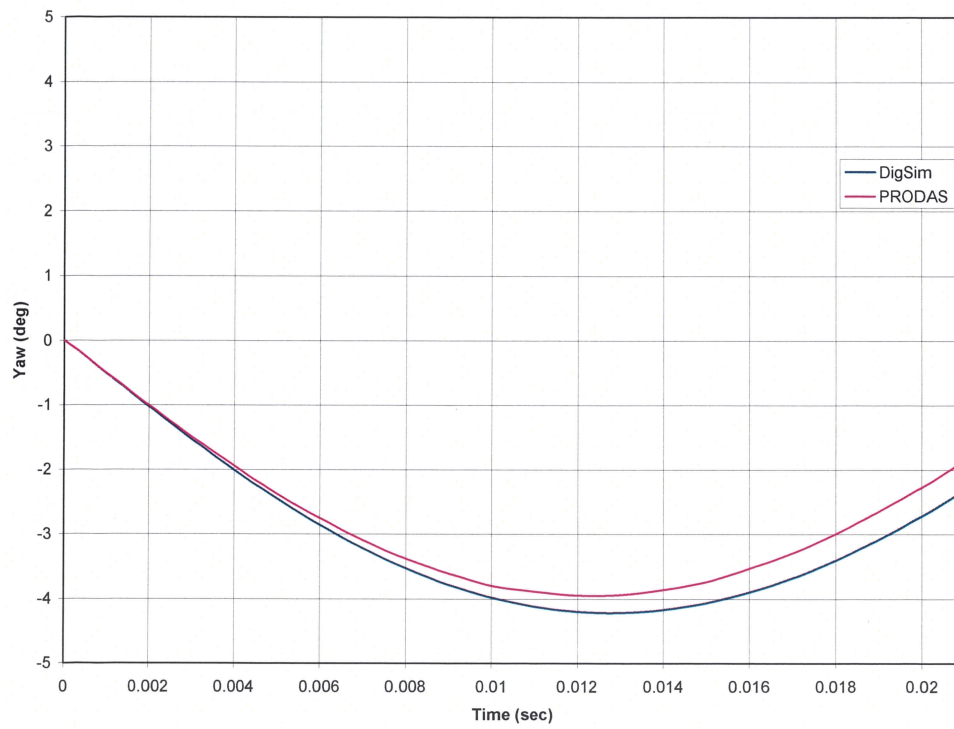


Figure 3.1 Baseline Projectile Yaw vs. Time Predicted by DigSim and PRODAS



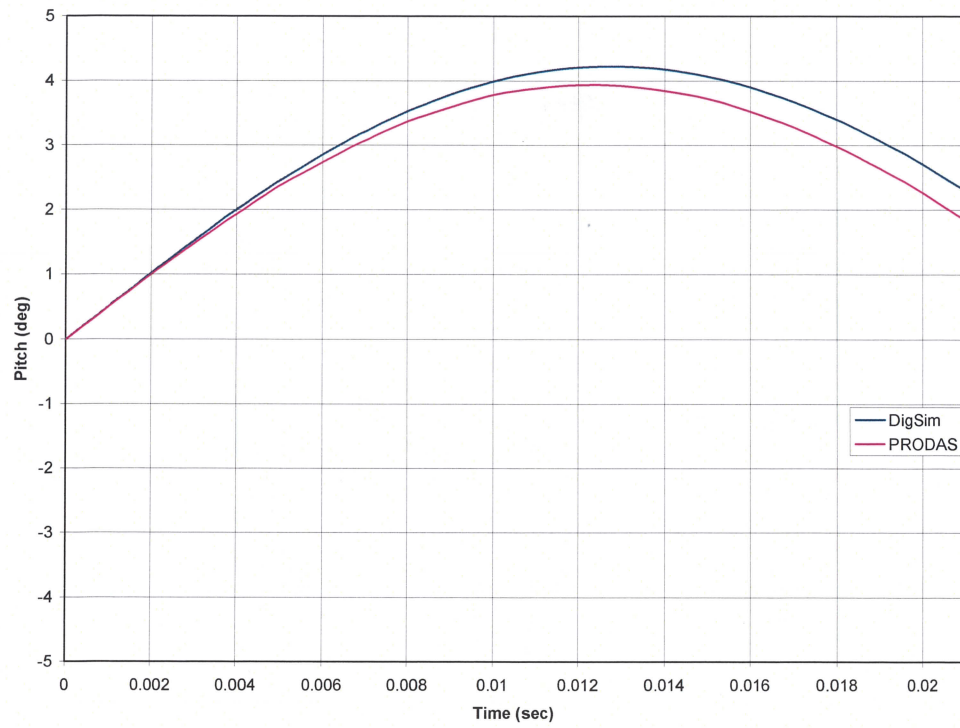


Figure 3.2 Baseline Projectile Pitch vs. Time Predicted by DigSim and PRODAS

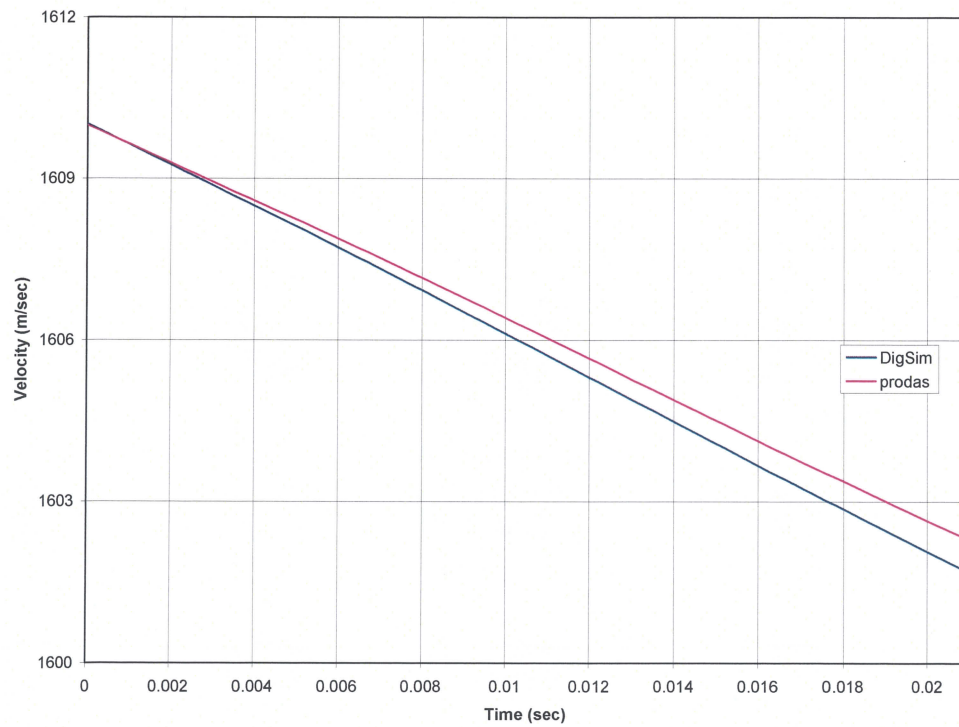


Figure 3.3 Baseline Projectile Velocity vs. Time Predicted by DigSim and PRODAS

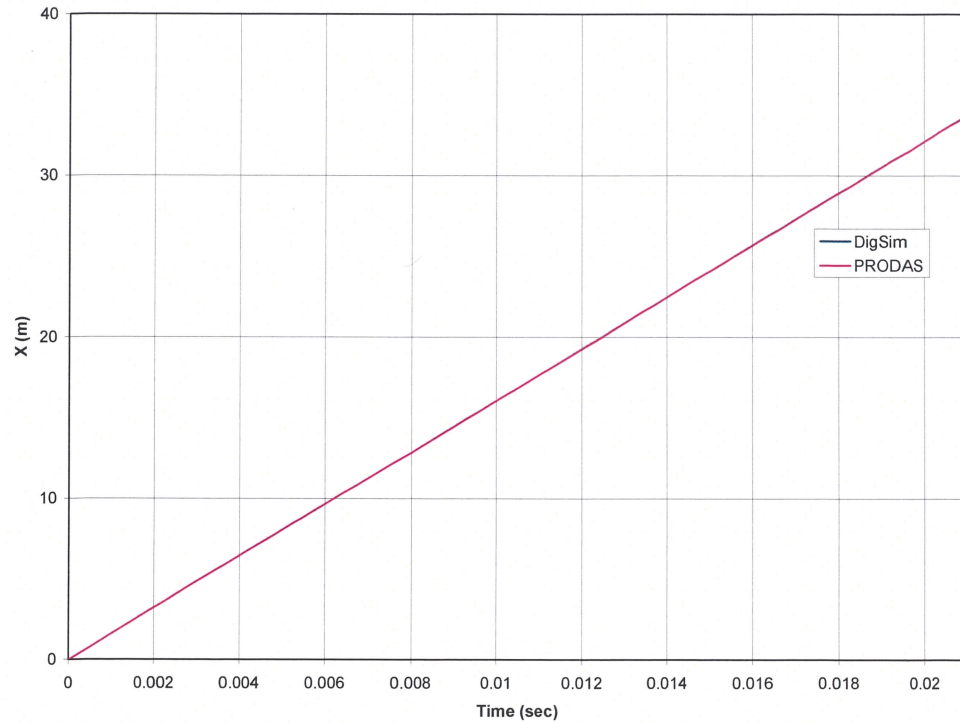


Figure 3.4 Baseline Projectile X-distance vs. Time Predicted by DigSim and PRODAS

Next, the PRODAS FINNER aerodynamics were used in DigSim. Figures 3.5 through 3.8 show the comparisons of trajectory predictions. The yaw and pitch angles differ by no more than 0.15 degrees throughout the flight time. Similar close agreement is seen between the velocity and X position predictions. These are the four key parameters analyzed when trying to predict the ARC baseline LGG test.

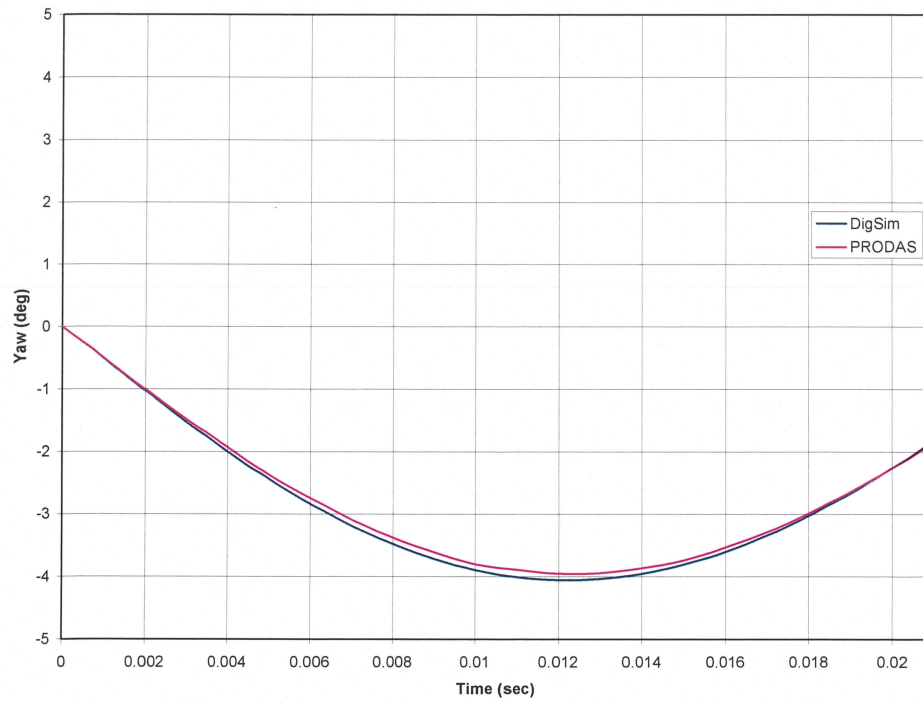


Figure 3.5 Baseline Projectile Yaw vs. Time Predicted by Modified DigSim and PRODAS

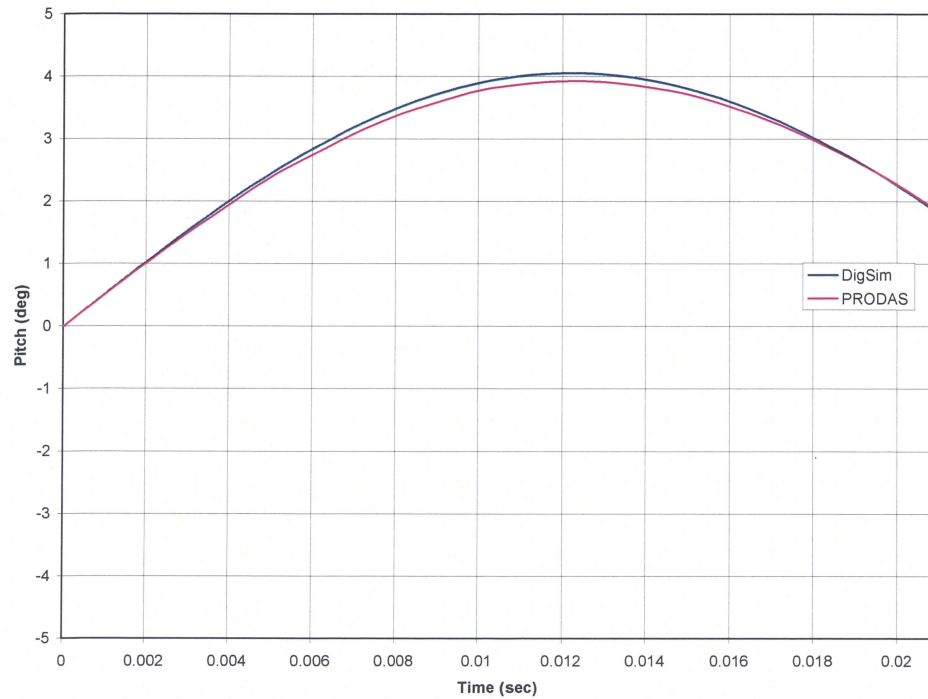


Figure 3.6 Baseline Projectile Pitch vs. Time Predicted by Modified DigSim and PRODAS

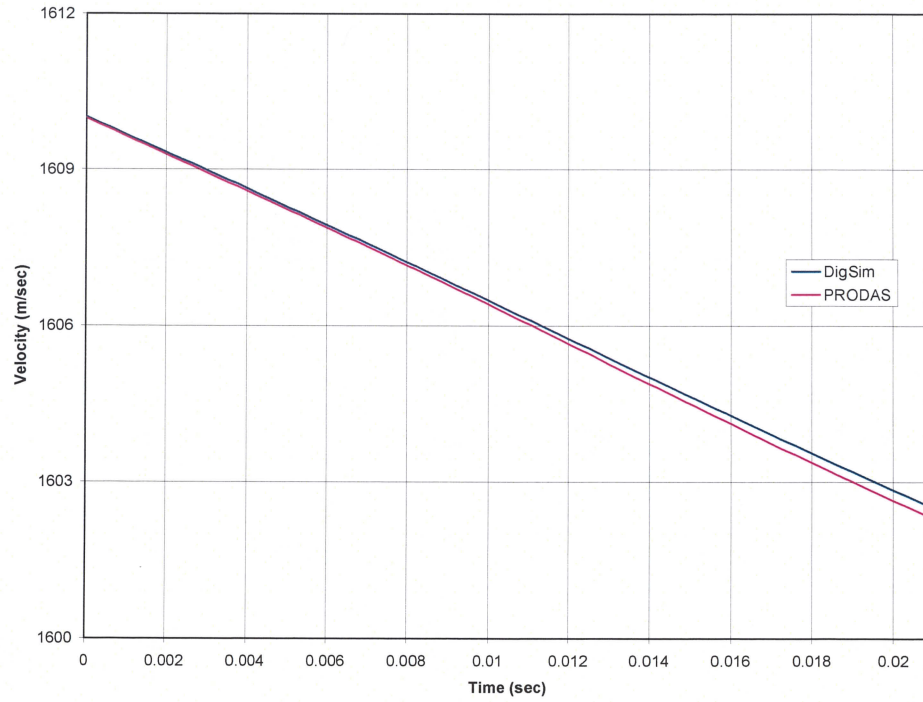


Figure 3.7 Baseline Projectile Velocity vs. Time Predicted by Modified DigSim and PRODAS

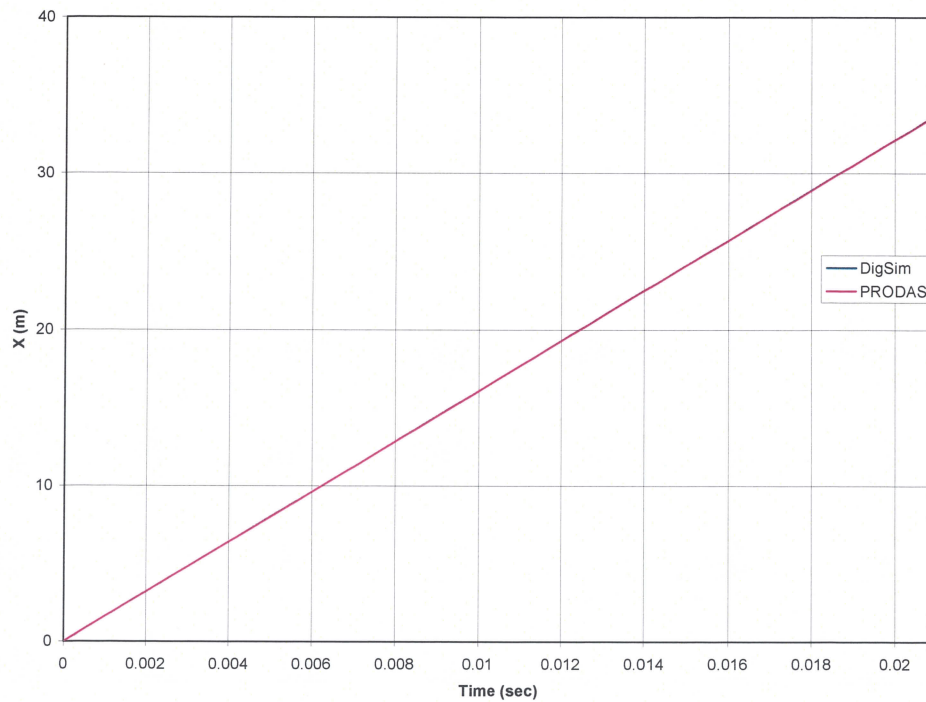


Figure 3.8 Baseline Projectile X-distance vs. Time Predicted by Modified DigSim and PRODAS



Based on the closeness of the predicted data from PRODAS and DigSim, the decision was made to use DigSim to verify the helium similarity in PRODAS. Thus, the next step was to run DigSim using helium and compare predictions to the ARC 0430 LGG test.

### *3.2 Predicting the LGG Test using DigSim*

The first step in trying to predict the 0430 LGG test using DigSim was to input all the known parameters from the test. These parameters consisted of pressure, temperature, and projectile velocity along with the mass properties and aerodynamics of the model. An example input file is shown in the Appendix. The only unknown inputs were the pitch and yaw tip-off rates. The ARC range does not have the capability to measure these parameters. Thus an iterative process was used to determine what tip-off rates produced the pitch and yaw attitude indicated in the baseline ARC 0430 LGG test data.

Figure 3.9 shows the break screen before and after the 0430 test used to trigger the x-ray images shown in Figures 3.10 and 3.11. Based on the hole size the projectile did not fly straight. Figures 3.10 and 3.11 show the projectiles pitch and yaw attitude just before impact. Neither angle meets the desired  $2^\circ$  requirement. Film cassettes are placed along the flight path to obtain the x-ray images. The two images in Figures 3.10 and 3.11 were taken about 0.61 meters from impact (33.53 m). They were setup such that the x-ray reticules are lined up parallel to the shot line using benchmarks and the ARC optical scope. Once the shot was complete, the x-rays were scanned, corrected for

magnification, and put into Photoshop® to measure the angle between the lines on the model with the reticules. This is usually done within a  $\pm 0.3^\circ$  accuracy depending on the resolution of the x-ray. The pitch and yaw angles measured at 0.61 m were assumed to be the impact orientation. Figure 3.12 shows the impact plate before and after the test. One can clearly see that the projectile didn't impact the metal plate at a small angle.

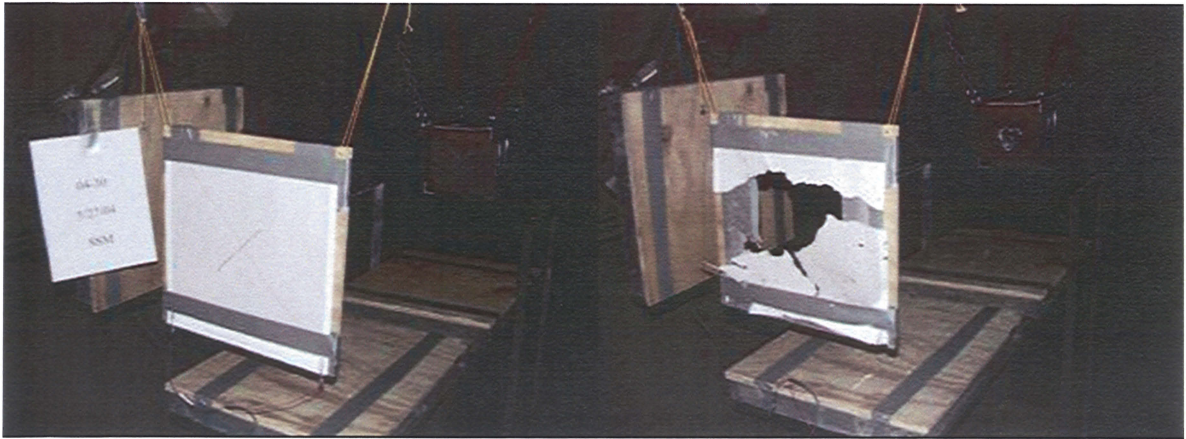


Figure 3.9 Break Screen Before and After 0430 LGG test

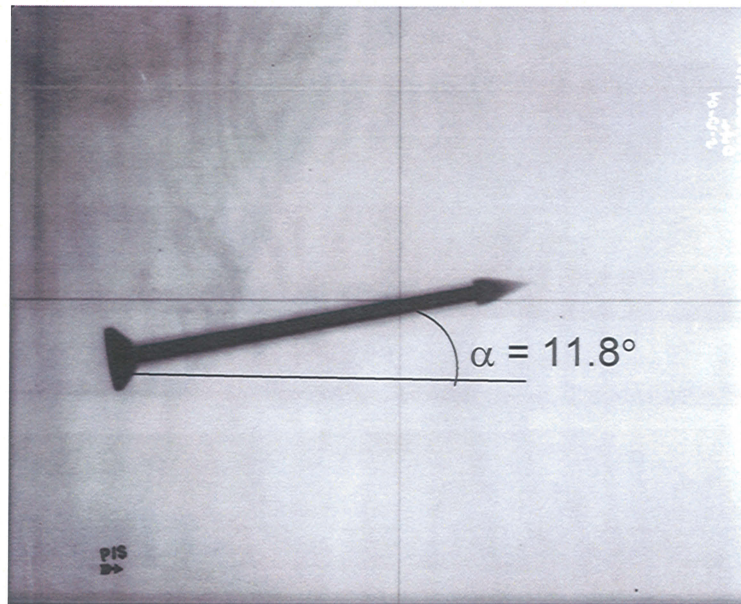


Figure 3.10 X-ray Image of Pitch for ARC 0430 LGG Test



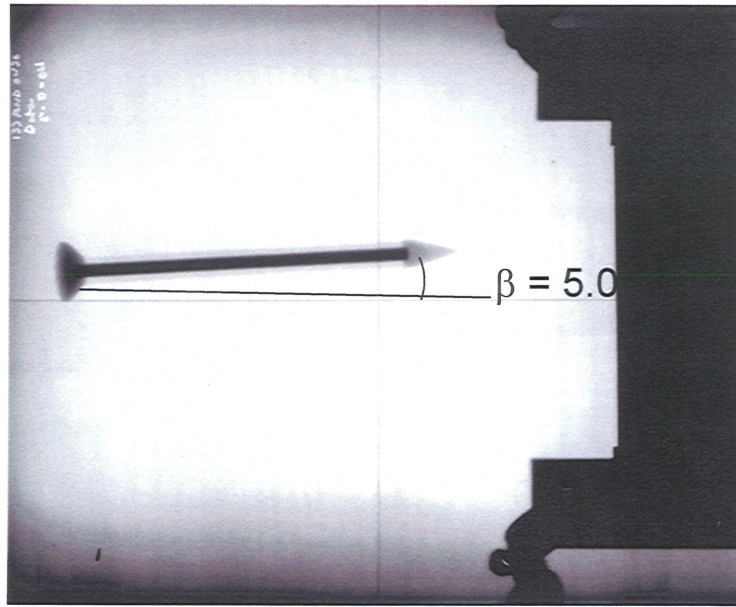


Figure 3.11 X-ray Image of Yaw for ARC 0430 LGG Test



Figure 3.12 Impact Point Before and After 0430 LGG Test

On average, the flight time for an ARC LGG shot is 21 milliseconds from muzzle launch to impact. Figures 3.13 through 3.16 show yaw, pitch, velocity, and flight distance predicted by DigSim for the 0430 LGG inputs. It was determined that a pitch tip-off rate of 11.85 rad/sec and a yaw tip-off rate of 5.05 rad/sec were needed in order to match the  $5^\circ$  yaw and  $11.8^\circ$  pitch attitude at impact (33.53 m downrange). This may

seem a bit large, but projectile launch always causes a lateral disturbance and therefore angular motion. Within the gun, attitude levels are normally low, but the angular rates can be greater than 5 rad/sec. This is amplified by the sabot separation [11]. As seen in the plots, at 21 milliseconds, yaw is about 4.97 degrees, pitch is around 11.79 degrees, velocity is around 1608 m/sec, and X-distance is about 33.63 meters downrange.

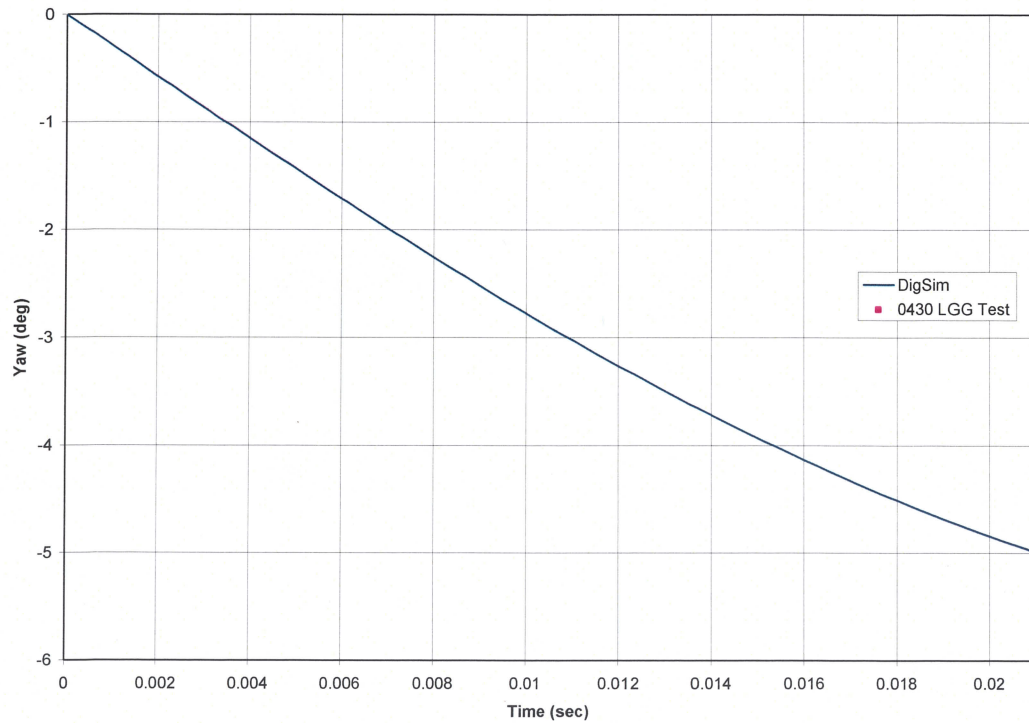


Figure 3.13 Baseline Projectile Yaw vs. Time Predicted by DigSim



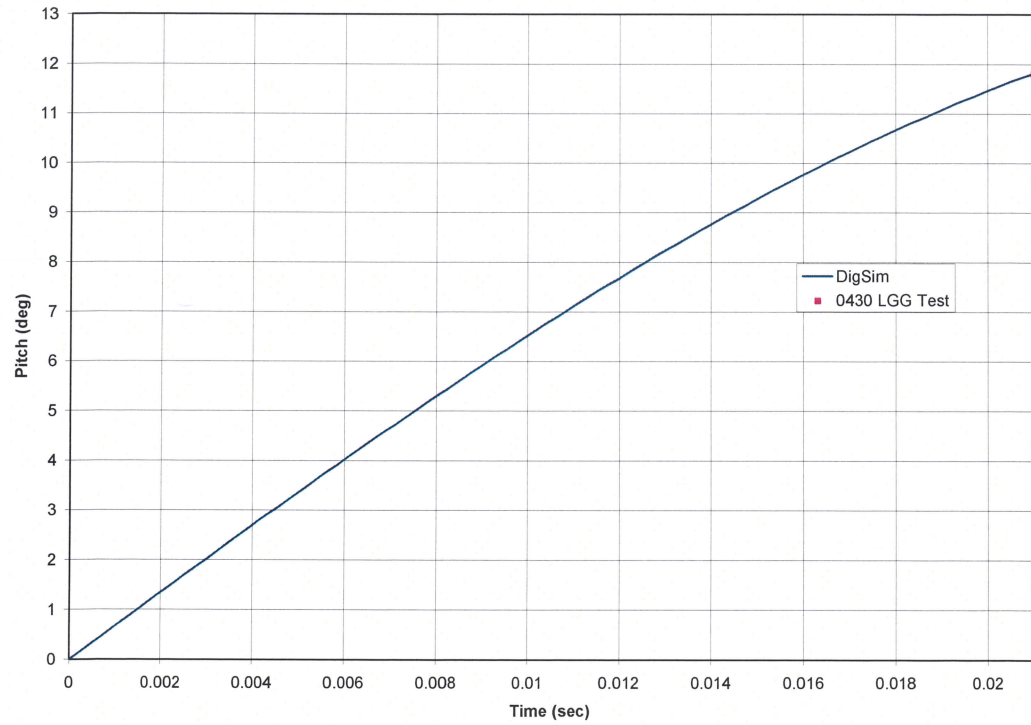


Figure 3.14 Baseline Projectile Pitch vs. Time Predicted by DigSim

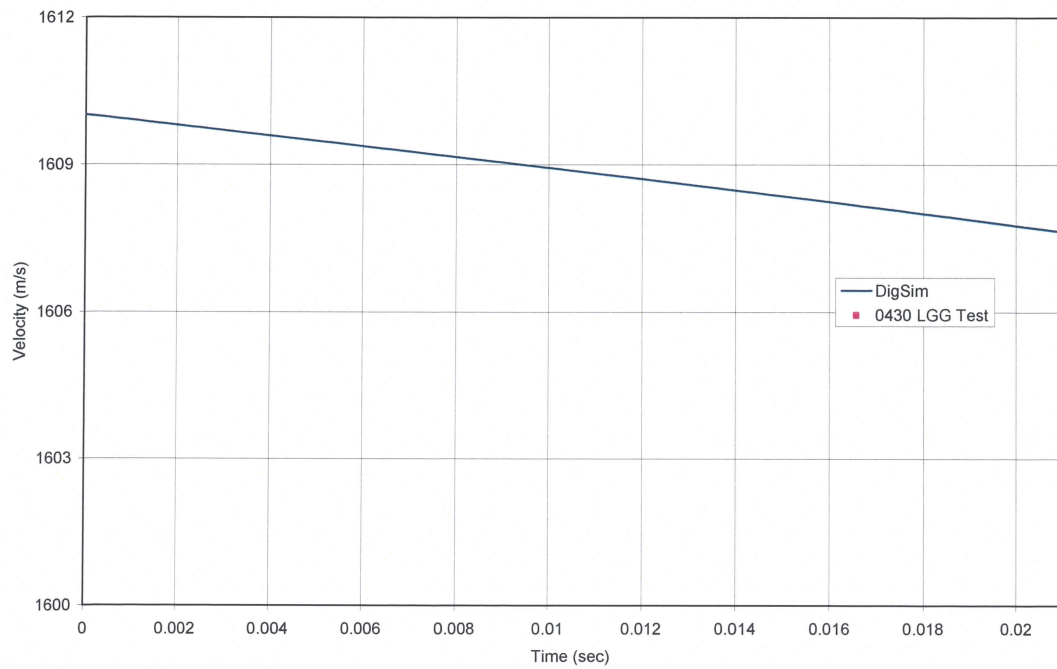


Figure 3.15 Baseline Projectile Velocity vs. Time Predicted by DigSim

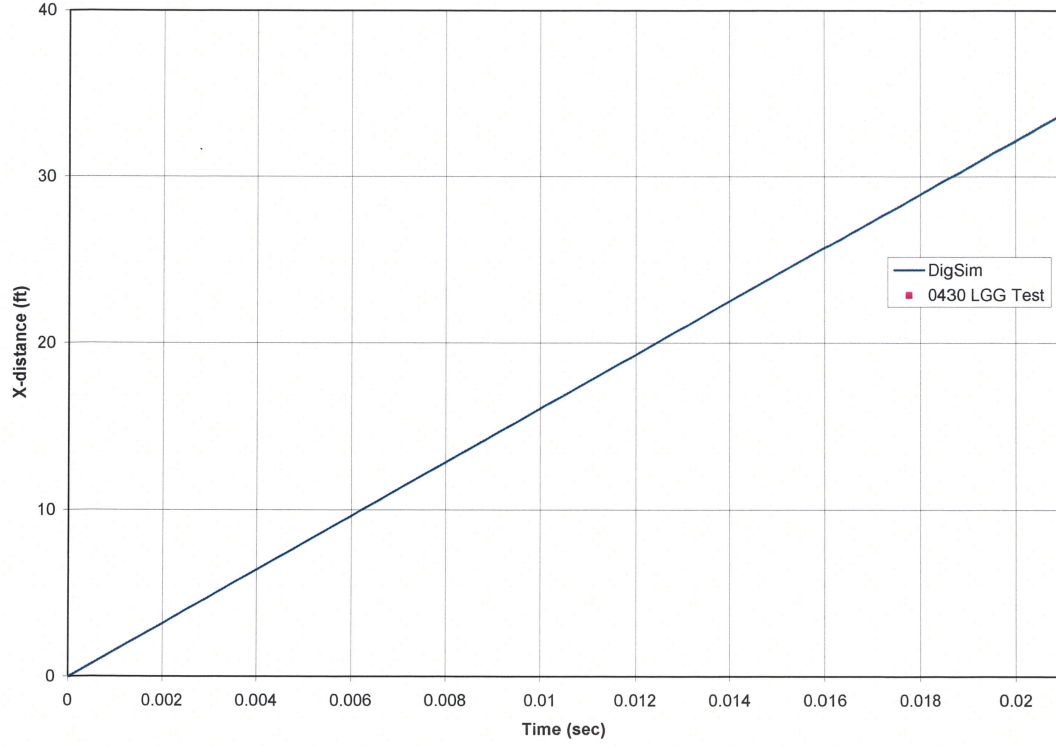


Figure 3.16 Baseline Projectile X-distance vs. Time Predicted by DigSim

### 3.3 Predicting LGG Test using PRODAS

Once the tip-off rates were determined using DigSim the next step was to use PRODAS to simulate the 0430 LGG test. Many attempts were made to use Mach, Froude, and Reynolds number scaling [12] to use an air atmosphere in PRODAS to mimic flight in a helium atmosphere. These classical scaling parameters are defined by

$$M = \frac{V}{a}, \quad (3.1)$$

$$Fr = \frac{V^2}{lg}, \quad (3.2)$$

$$\text{Re} = \frac{\rho V d}{\mu}, \quad (3.3)$$

where  $V$  is velocity,  $a$  is the speed of sound,  $l$  and  $d$  are characteristic lengths,  $g$  is gravity,  $\rho$  is density, and  $\mu$  is viscosity. The first step was to match the Mach Number of air and Helium to determine the velocity to use in PRODAS. Substituting the Helium test values into the Mach Number equation (3.1) yielded the air velocity to be,

$$V_{air} = V_{He} \sqrt{\frac{\gamma_{air} R_{air} T}{\gamma_{He} R_{He} T}}. \quad (3.4)$$

Using the 0430 baseline test day helium conditions ( $V=1610\text{m/s}$ ,  $T=300\text{K}$ ) the velocity for PRODAS was determined in air to be  $547.96\text{ m/s}$ . This value was used in the Froude equation (3.2) to determine the characteristic length to use in PRODAS. Substituting the Helium values into the Froude equation (3.2) yielded the air characteristic length to be,

$$l_{air} = l_{He} \left( \frac{V_{air}}{V_{He}} \right)^2. \quad (3.5)$$

The mid-body length of  $155.37\text{ mm}$  was chosen from the baseline test and the PRODAS mid-body length was determined to be  $17.99\text{ mm}$ . This length was used to scale the nose and tail dimensions to use in PRODAS. The nose shortened from  $23.7\text{ mm}$  to  $2.75\text{ mm}$ , and the tail shortened from  $10.8\text{ mm}$  to  $1.25\text{ mm}$ . Therefore, the total length went from  $189.87\text{ mm}$  to  $21.99\text{ mm}$ . The mass went from  $71.8\text{ grams}$  to  $5.73\text{ grams}$  for the scaled model. When using this approach the PRODAS *Aerodynamics Stability Evaluation* failed because the CP of the model was ahead of the CG. Figure 3.17 shows the *Stability Evaluation* screen with a negative static margin for the scaled model.

The mid-body diameter of 12.7 mm was next used as the characteristic length in the Froude equation (3.2) to scale the baseline model using the same velocity of 547.96 m/s obtained from equation 3.4. The PRODAS mid-body diameter was determined to be 1.47 mm, and the tail diameter was 3.23 mm. The mass became 0.96 grams. The length of the model remained the same. Figure 3.18 shows the *Stability Evaluation* screen for the scaled model. The model is stable, but due to the velocity being much lower it only flew a distance of 11.48 meters. The pitch and yaw attitudes of 12.16° and 5.29°, respectively, were also slightly higher than the baseline.

Reynolds number scaling using the scaled velocity of 547.96 m/s calculated from equation 3.4 and a temperature of 300 K was also attempted. A characteristic length for PRODAS was determined using equation 3.3. Substituting the Helium values into the Reynolds Number equation (3.3) yielded the air characteristic length to be,

$$l_{air} = l_{He} \left( \frac{\rho_{He}}{\rho_{air}} \right) \left( \frac{V_{He}}{V_{air}} \right) \left( \frac{\mu_{air}}{\mu_{He}} \right). \quad (3.6)$$

This was used to scale the model based on total length and then based on diameter. The PRODAS *Stability Evaluation* indicated both had the CP ahead of the CG and therefore, neither of the scaled models was stable.



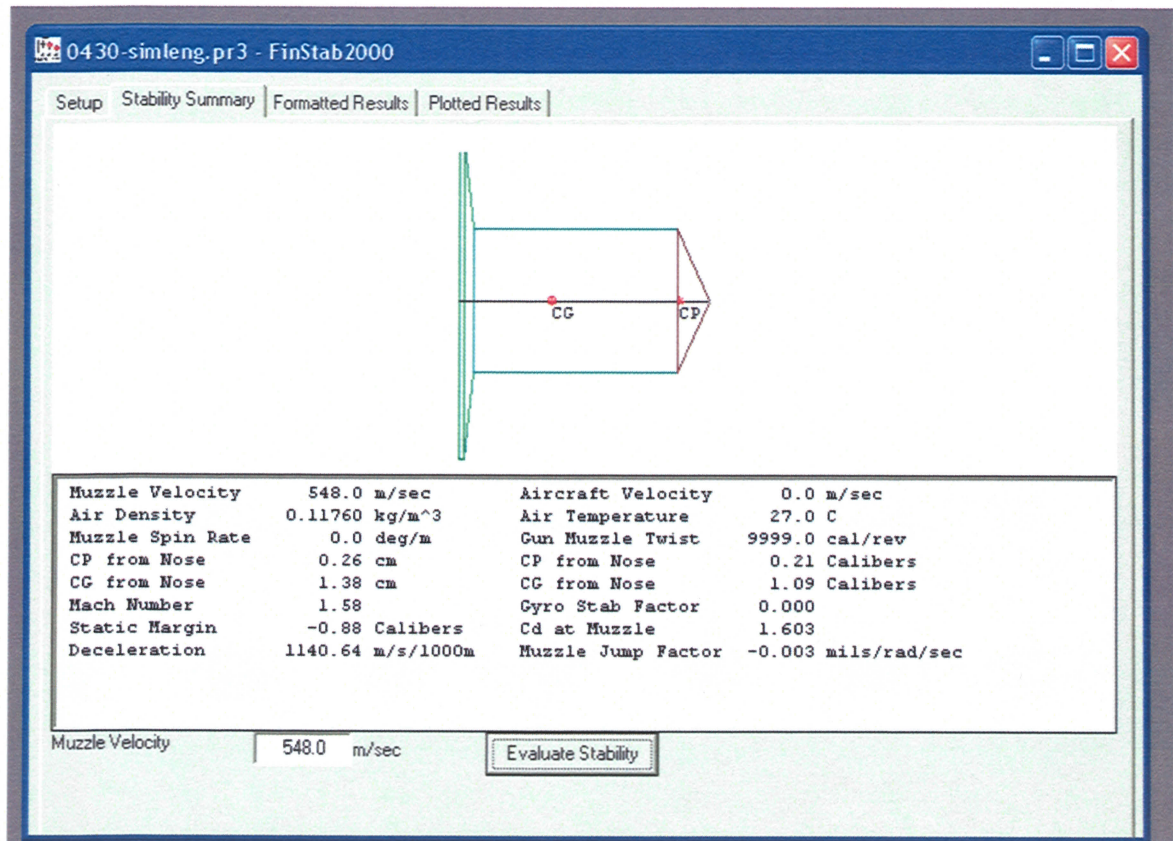


Figure 3.17 PRODAS Stability Evaluation Screen for *M-Fr* Mid-body Scaled Model [6]

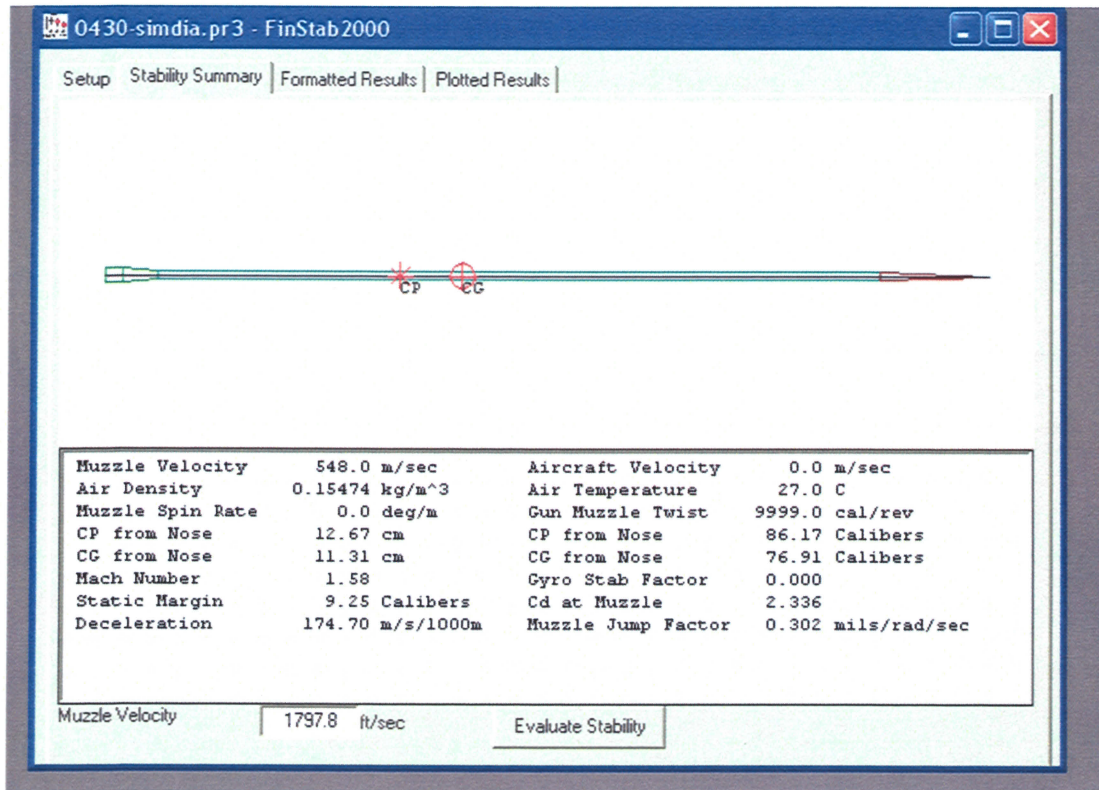


Figure 3.18 PRODAS Stability Evaluation Screen for *M-Fr* Diameter Scaled Model [6]

It became evident that traditional scaling approaches were not adequate. The resulting scaled models were either unstable or yielded completely unacceptable flight profiles. A simple approach to scaling was next attempted using a modified Ideal Gas equation

$$P_{air} = \rho_{air} R_{air} T_{air} = P_{He} = \rho_{He} R_{He} T_{He} . \quad (3.7)$$

Assuming the helium temperature and density to be the same as air yielded the air pressure to be,

$$P_{air} = \rho_{He} R_{air} T_{He} . \quad (3.8)$$

Substituting the Helium density,

$$\rho_{He} = \frac{P_{He}}{R_{He} T_{He}}, \quad (3.9)$$

reduced the air pressure equation to

$$P_{air} = \frac{P_{He}}{7.237}. \quad (3.10)$$

This approach didn't require any geometric changes to be made to the model used for the LGG test. Table 3.1 shows the property data used and the resulting air pressure run in PRODAS to simulate the baseline helium LGG test. A much smaller equivalent air pressure is required to match the baseline test helium density. This is due to the helium gas constant being so large relative to air.

Table 3.1 Modified Equation of State Property Data

	Pressure (Pa)	Temperature (K)	Gas Constant (J/KgK)
Air (Simulated Helium)	1842	300	287
Helium	13332	300	2077

Using the calculated pressure of 1842 Pa and tip-off rates of 11.85 rad/sec and 5.05 rad/sec for pitch and yaw, respectively, PRODAS was run to determine if it would predict the DigSim results adjusted to match the 0430 LGG test. The test velocity of 1610 m/sec was used in the PRODAS run yielding a higher Mach Number (4.64) than DigSim (1.58) because the gas constant for air ( $R_{air}$ ) was still being used. But this gave the proper flight distance needed to match the LGG test.



Figures 3.19 through 3.21 show predicted pitch, yaw, and distance for the pressure adjusted air PRODAS simulation versus DigSim with the actual helium atmosphere. The PRODAS simulation is extremely close to DigSim. Table 3.2 compares the numerical values for pitch, yaw, and distance at 21 milliseconds from the DigSim and PRODAS simulations to test data. There is less than 1% difference in the predicted pitch and distance values, and less than 4% in the yaw values. The predicted attitudes are well within the  $\pm 0.3^\circ$  measurement error of the range.

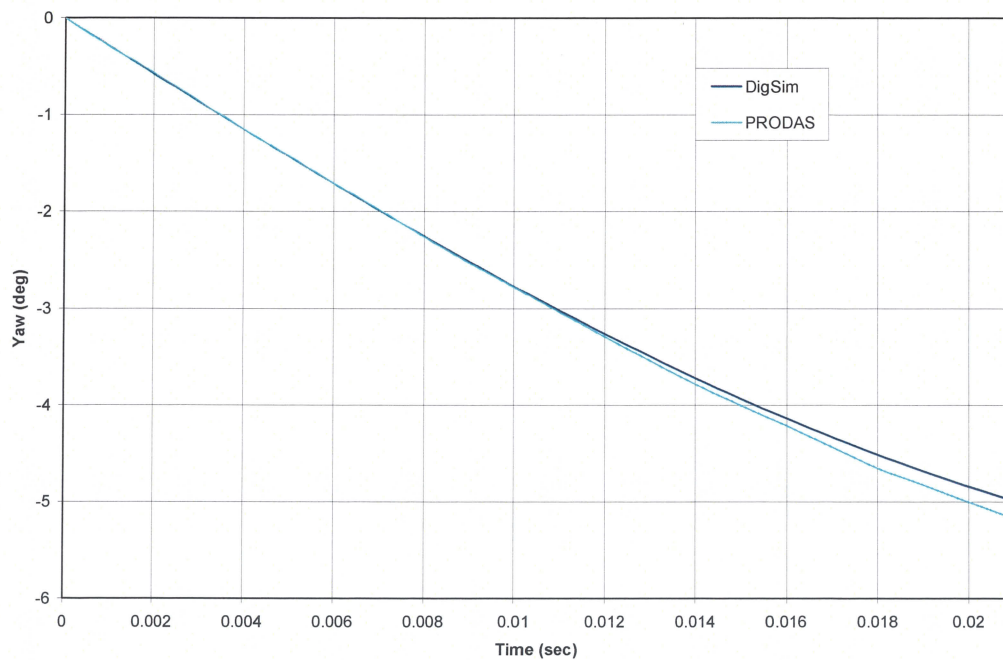


Figure 3.19 Yaw vs. Time for Simulated Helium in PRODAS



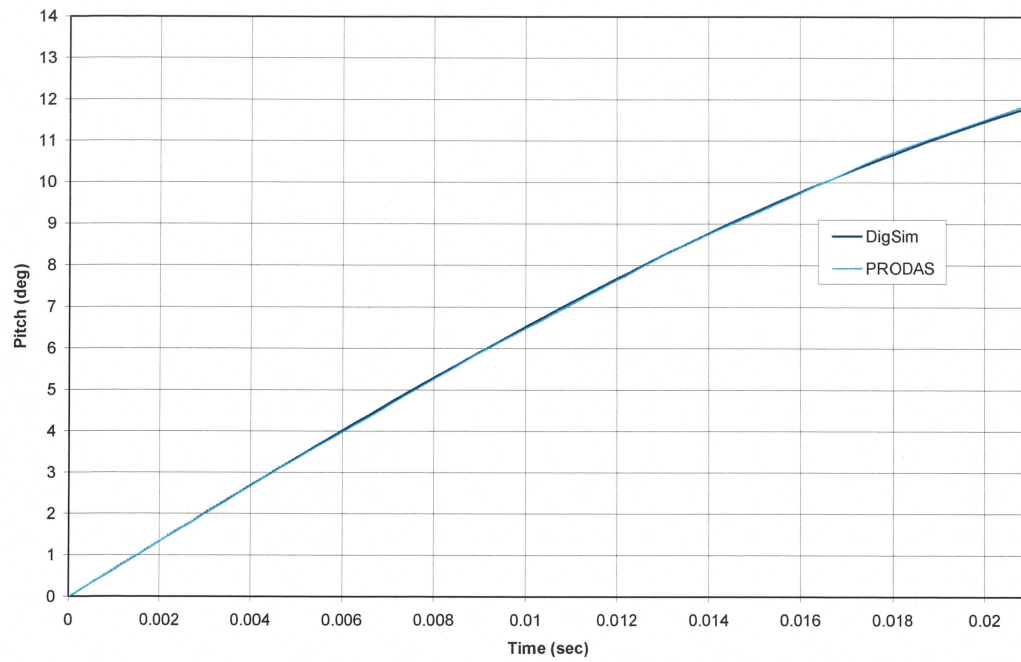


Figure 3.20 Pitch vs. Time for Simulated Helium in PRODAS

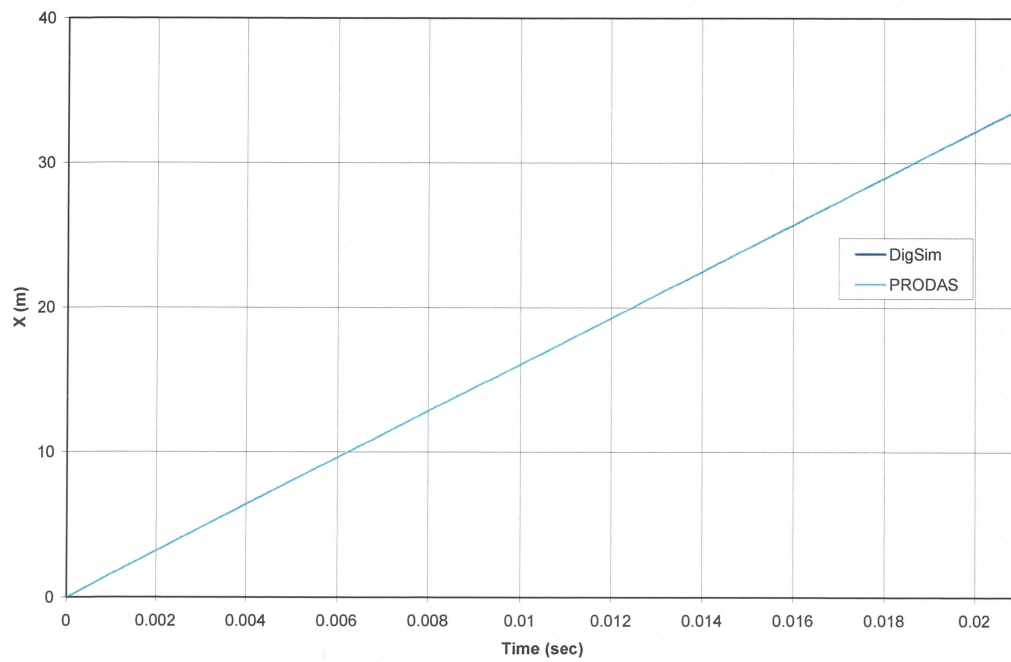


Figure 3.21 X-distance vs. Time for Simulated Helium in PRODAS

Table 3.2 Baseline Projectile Simulation Attitude and Distance Comparison

	Velocity (m/s)	Pitch (deg)	Yaw (deg)	X-dist (m)
DigSim	1610	11.79	-4.97	33.63
PRODAS	1610	11.90	-5.17	33.81
Actual	1610	11.80	-5.0	33.53

Figures 3.22 and 3.23 show the effects of air and simulated Helium, using the same conditions (velocity, temperature, etc.), on the predicted trajectory in PRODAS. The frequency of oscillations is much slower for the simulated Helium and the magnitudes are more than doubled. This is due to the density of Helium being about 7 times less than the density of air.

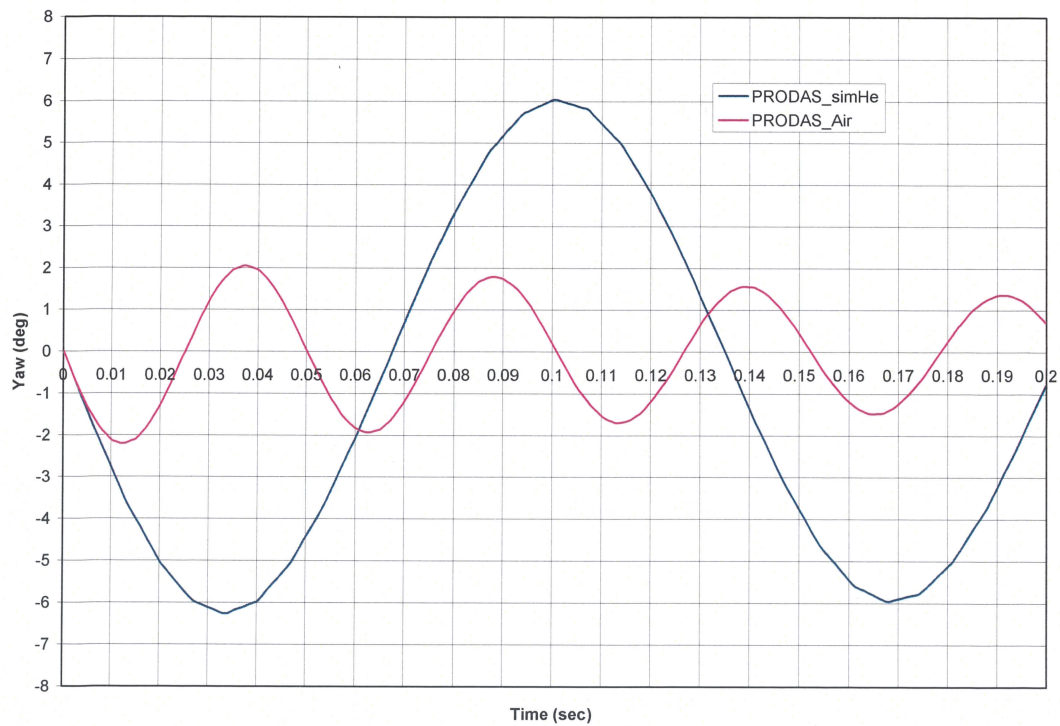


Figure 3.22 Yaw vs. Time for Air and Simulated Helium in PRODAS

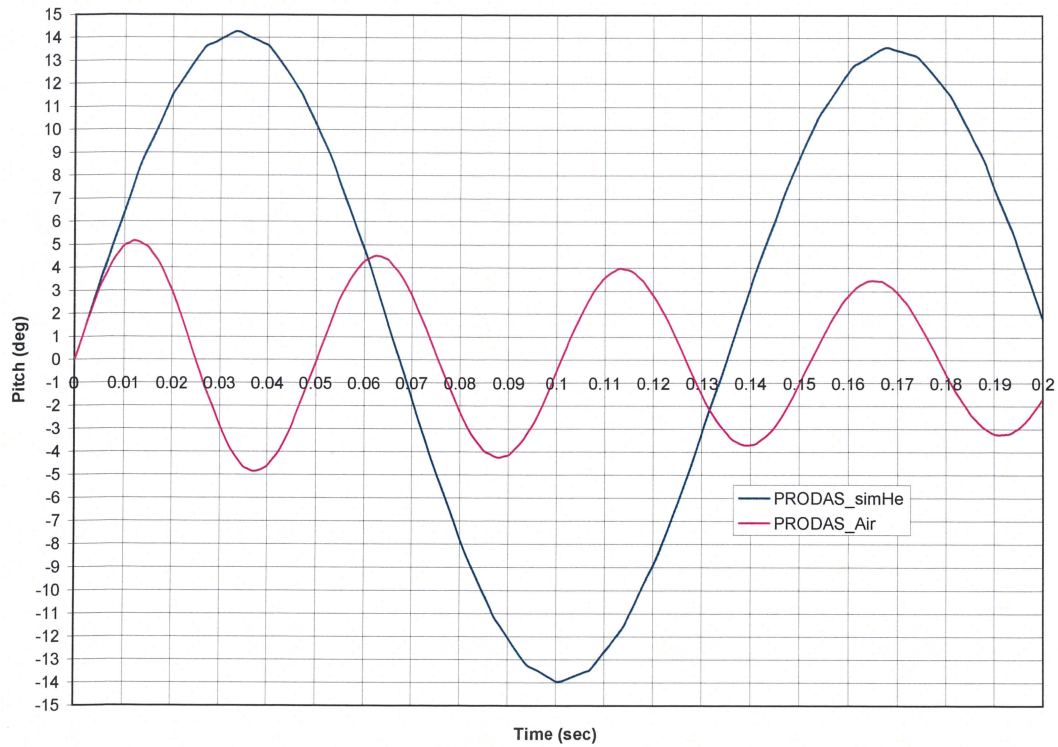


Figure 3.23 Pitch vs. Time for Air and Simulated Helium in PRODAS

### 3.4 Predicting Pitch and Yaw Limit in PRODAS

Using the tip-off rates (11.85 rad/sec pitch and 5.05 rad/sec yaw) and velocity (1610 m/s) from the PRODAS scaling study, the next step was to determine what scaled pressure was needed to meet the 2° pitch and yaw attitude for the ARC gun range. From the initial analysis, it was noticed that if the actual helium pressure of 13.33 kPa was used in the PRODAS simulation with air, the yaw attitude of 1.04° was below the 2° limit while the pitch attitude of 2.43° exceeds it. Using the pressure scaling from Section 3.3 and equation 3.10, this would mean a pressure of 96.47 kPa for the actual helium LGG test. Using a slightly higher pressure in PRODAS of 14 kPa (101.32 kPa for LGG), the predicted pitch was still over the 2° limit by 0.09°. But because the pitch was within the

measurement accuracy ( $\pm 0.3^\circ$ ) of the ARC, the 14 kPa pressure was used for the RSM analysis.



## CHAPTER FOUR

### OPTIMUM PROJECTILE DESIGN

The previous chapter demonstrated that PRODAS with an air atmosphere could be used with pressure scaling to reasonably predict LGG projectile flight in helium. The next step was to determine the optimum projectile design that would meet the maximum 2° attitude requirement. In this chapter Response Surface Methodology (RSM) introduced in Chapter 2 is used to aid in the process.

#### *4.1 Projectile Design Matrix*

For the Face Centered Cube Design (FCD) discussed in Chapter 2, RSM requires 3 independent variables for analysis. For this study, the projectile nose cone angle, tail flare angle, and body length were chosen. As discussed in Chapter 2, a high, nominal, and low value is required for each variable to achieve a more even affect on the response. Table 4.1 shows the physical value ranges used for the RSM Analysis.

Table 4.1 Range of Independent Projectile Design Variables

	Tail Angle (deg)	Mid-Body Length (mm)	Cone Angle (deg)
High	50	171.04	20
Nominal	45	155.37	15
Low	40	139.7	10

Using the Table 4.1 variables, a PRODAS RSM run matrix was established as shown in Table 4.2. Equation 2.7 was used to determine the coded variable values as shown in Table 2.1, repeated here as Table 4.3. For the RSM run matrix 1 represents the High value, 0 represents the Nominal, and -1 represents the Low value. Since this is a  $2^k$  design using three variables, the first eight runs define the first-order RSM equation, and the last seven are used to develop the second-order RSM equation.

Table 4.2 PRODAS RSM Run Matrix

Run	Tail Angle (deg)	Mid-Body Length (mm)	Cone Angle (deg)	Total Projectile Length (mm)
1	40	139.7	10	187.97
2	50	139.7	10	185.29
3	40	171.04	10	222.49
4	50	171.04	10	216.63
5	40	139.7	20	169.41
6	50	139.7	20	166.72
7	40	171.04	20	200.75
8	50	171.04	20	198.06
9	50	155.37	15	188.64
10	40	155.37	15	191.33
11	45	171.04	15	205.54
12	45	139.7	15	174.19
13	45	155.37	20	183.62
14	45	155.37	10	202.18
15	45	155.37	15	189.87

Table 4.3 PRODAS Coded RSM Run Matrix

Run	Tail Angle	Mid-Body Length	Cone Angle
1	-1	-1	-1
2	1	-1	-1
3	-1	1	-1
4	1	1	-1
5	-1	-1	1
6	1	-1	1
7	-1	1	1
8	1	1	1
9	1	0	0
10	-1	0	0
11	0	1	0
12	0	-1	0
13	0	0	1
14	0	0	-1
15	0	0	0

#### 4.2 PRODAS/RSM Run Matrix Results

Using the run matrices of Tables 4.2 and 4.3, PRODAS runs were made with the various lengths and angles. All the runs used the same velocity (1610 m/s), tip-off rates (11.85 rad/sec pitch and 5.05 rad/sec yaw), temperature (300K), and scaled pressure (14kPa) determined from the initial analysis of the 0430 baseline LGG shot in order to meet the maximum 2° attitude requirement.

Table 4.4 shows the results for the run matrix. It shows that all the runs fall under the 2° requirement for yaw, but only five of the runs are under this limit for pitch. There was minimum effect on the flight (downrange) distance. All the runs meet the 33.54 meters. Run 15 represents the nominal run. It basically lies in the middle of the matrix. Runs 9 and 14 are almost the same as the nominal. This is most likely due to using the same length for the projectile. Simple observation of the predicted data



indicates that the runs made using the same body length are very similar. The smallest body length of 139.7 mm (-1 coded) produced the smallest pitch and yaw attitude. While the longest body length of 171.044 mm (+1 coded) produced the largest values for pitch and yaw attitude.

Table 4.4 PRODAS RSM Run Matrix Results

Run	Tail Angle	Mid-Body Length	Cone Angle	pitch (deg)	yaw (deg)	X-distance (m)	Both Attitudes Under Req
1	-1	-1	-1	1.5	-0.64	33.72	yes
2	1	-1	-1	1.21	-0.52	33.72	yes
3	-1	1	-1	2.98	-1.27	33.73	no
4	1	1	-1	2.87	-1.23	33.73	no
5	-1	-1	1	1.68	-0.72	33.7	yes
6	1	-1	1	1.33	-0.57	33.7	yes
7	-1	1	1	3.17	-1.35	33.72	no
8	1	1	1	3.02	-1.29	33.72	no
9	1	0	0	2.08	-0.89	33.72	no
10	-1	0	0	2.28	-0.97	33.72	no
11	0	1	0	2.87	-1.22	33.73	no
12	0	-1	0	1.26	-0.54	33.71	yes
13	0	0	1	2.22	-0.94	33.71	no
14	0	0	-1	2.07	-0.88	33.73	no
15	0	0	0	2.09	-0.89	33.72	no

#### 4.3 RSM Analysis

One of the benefits of RSM analysis is that the coefficients in the resultant response equation can be used to determine which of the design variables or their combinations have the largest effect on the response. The data from the PRODAS runs was used to derive the second-order RSM response (equation 2.4). The resulting equations for pitch and yaw, respectively, are



$$y(\text{pitch}) = 2.086 - 0.11X_1 + 0.793X_2 + 0.079X_3 + 0.0475X_1X_2 - 0.0125X_1X_3 + 0.005X_2X_3, \quad (4.1)$$

$$+ 0.0025X_1X_2X_3 + 0.0944X_1^2 - 0.0206X_2^2 + 0.0594X_3^2$$

$$y(\text{yaw}) = -0.8869 + 0.045X_1 - 0.337X_2 - 0.033X_3 - 0.0213X_1X_2 + 0.00625X_1X_3 - 0.00125X_2X_3, \quad (4.2)$$

$$- 0.000125X_1X_2X_3 - 0.0439X_1^2 + 0.00611X_2^2 - 0.0239X_3^2$$

where  $y$  is the pitch/yaw attitude response,  $X_1$  is the coded tail flare angle,  $X_2$  is the coded length, and  $X_3$  is the coded cone angle. The RSM coefficient magnitudes are plotted in Figure 4.1. The larger the magnitude of the coefficient, the more the response depends on that variable or combination of variables. The average response is represented by  $\beta_0$ . The figure shows the projectile mid-body length ( $\beta_2$ ) had the most effect on the attitudes which is basically what was observed by simple inspection of the data. It also shows that the interaction between the mid-body length and cone angle ( $\beta_{23}$ ) along with the interaction of all three variables ( $\beta_{123}$ ) had very little to no effect on the attitudes.

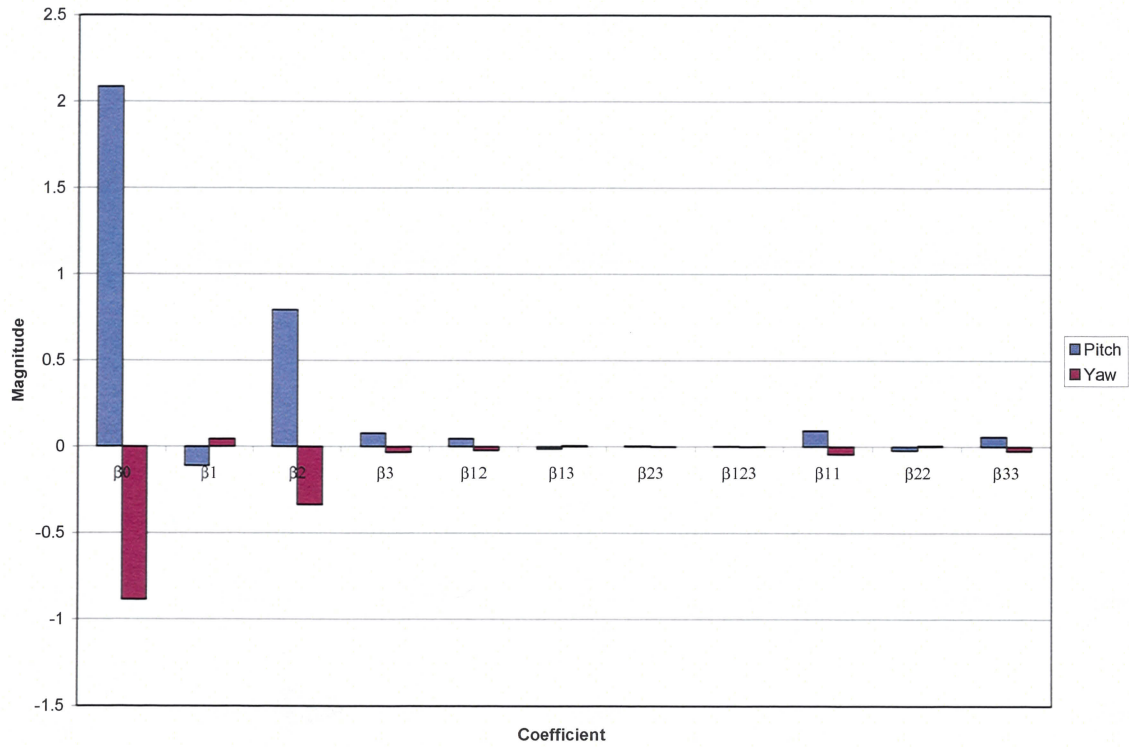


Figure 4.1 2<sup>nd</sup>-Order RSM Coefficients for Pitch and Yaw

The coded variables from Table 4.4 were applied to the derived RSM equations 4.1 and 4.2 to determine the pitch and yaw attitudes. The difference between the RSM predictions and PRODAS predictions, known as the Residual, was calculated by equation 2.6. The predicted pitch and yaw from PRODAS and RSM, along with the residuals, are shown in Table 4.5. Figure 4.2 shows a plot of the residuals (in degrees), and one can see that they are very small for each of the runs. The largest for pitch was  $0.013^\circ$  and yaw was  $0.006^\circ$ . None of the values are large enough to indicate problems with outliers in the data set. Because the residuals are so small for both attitudes, the RSM equations prove to be a good representation of the projectile motion. In other words, the RSM equations can be used in place of PRODAS to calculate the attitude for

other body geometries within the range studied here. If the residuals were large relative to the response, increasing the order of the equation and therefore the number of PRODAS runs would reduce the error in the curve-fit.

Table 4.5 PRODAS vs. RSM Attitudes

Run	PRODAS Pitch (deg)	RSM Pitch (deg)	Residual (deg)	PRODAS Yaw (deg)	RSM Yaw (deg)	Residual (deg)
1	1.5	1.495	0.005	-0.64	-0.639	-0.001
2	1.21	1.210	-0.0003	-0.52	-0.521	0.001
3	2.98	2.981	-0.001	-1.27	-1.270	0.0001
4	2.87	2.876	-0.006	-1.23	-1.233	0.003
5	1.68	1.673	0.007	-0.72	-0.717	-0.003
6	1.33	1.328	0.002	-0.57	-0.570	0.000
7	3.17	3.169	0.001	-1.35	-1.349	-0.001
8	3.02	3.024	-0.004	-1.29	-1.291	0.001
9	2.08	2.071	0.009	-0.89	-0.886	-0.004
10	2.28	2.291	-0.011	-0.97	-0.976	0.006
11	2.87	2.859	0.011	-1.22	-1.218	-0.002
12	1.26	1.273	-0.013	-0.54	-0.544	0.004
13	2.22	2.225	-0.005	-0.94	-0.944	0.004
14	2.07	2.067	0.003	-0.88	-0.878	-0.002
15	2.09	2.086	0.004	-0.89	-0.887	-0.003

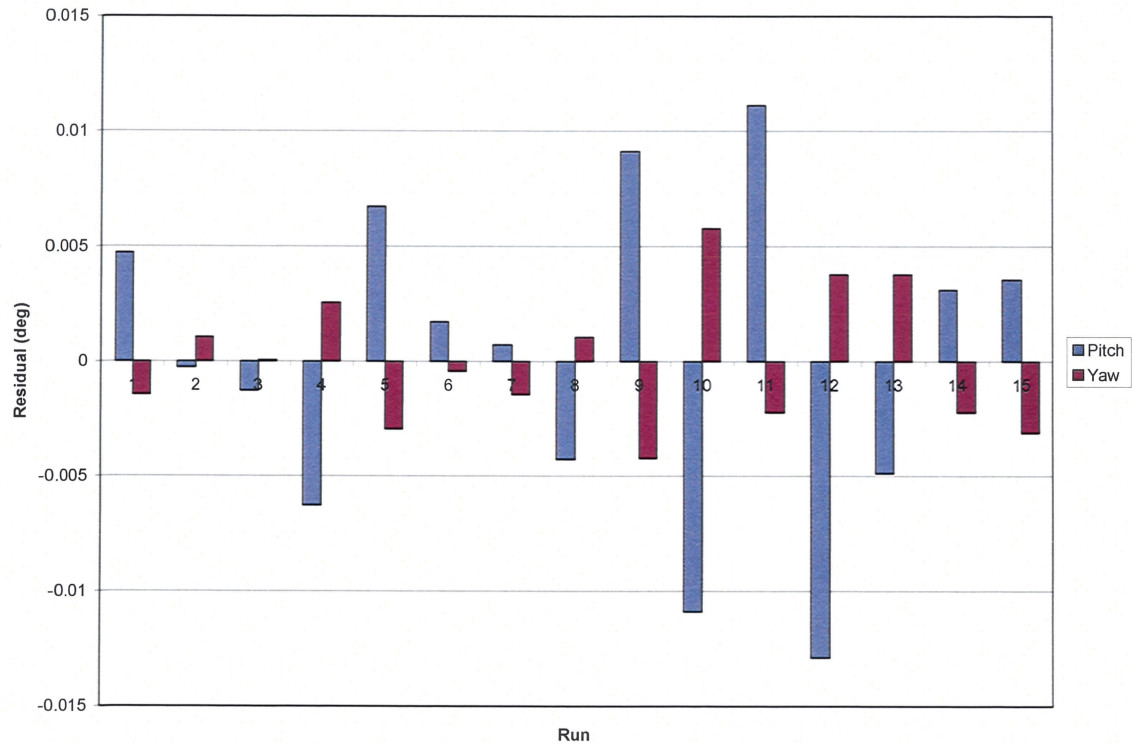


Figure 4.2 RSM Residuals for Pitch and Yaw

Although five of the projectile geometries produced flight attitudes under the maximum requirement for both pitch and yaw, the Run 2 configuration produced the minimum attitude angles. An iterative process could be used on the RSM equations to determine a geometric configuration that would give the absolute minimum values for the pitch and yaw attitude, but because the Run 2 results were well under the attitude requirement and measurement accuracy of the range, it was chosen to produce a new LGG shot at the ARC. RSM would be more useful in further analysis with a larger matrix of variables to determine their sensitivity.



## CHAPTER FIVE

### ARC LGG TEST

#### *5.1 ARC 133 LGG*

The UAH ARC has three Light Gas Guns ranging from a 254 mm diameter pump tube to 108 mm. The 133 mm gun used in this study is shown in Figures 5.1 and 5.2. This is a two-stage LGG consisting of pump tube, launch tube, and impact chamber. Table 5.1 gives the gun dimensions [1]. Figure 5.3 shows the 133 mm LGG range schematic.

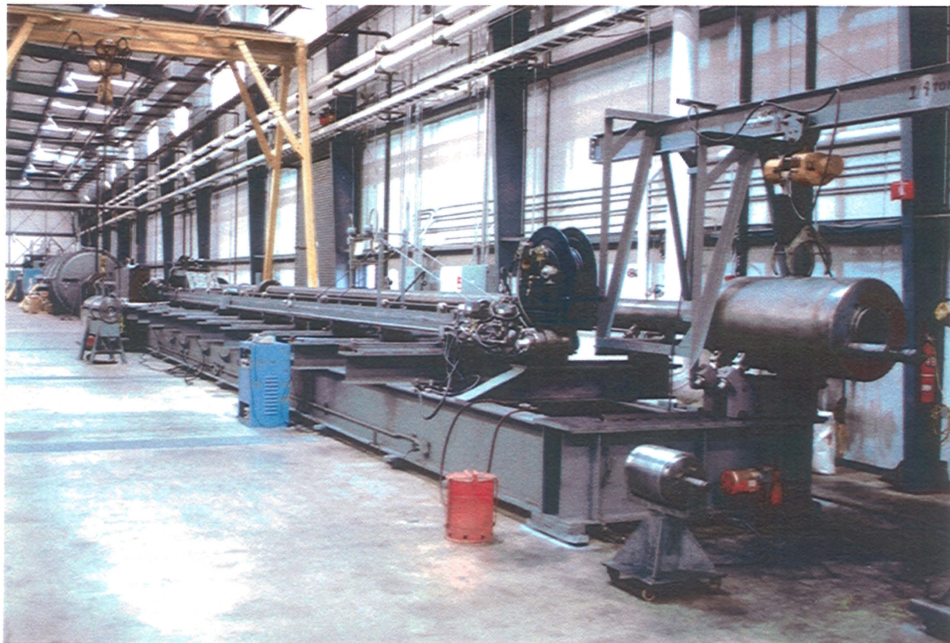


Figure 5.1 133 mm ARC LGG Pump and Launch Tube

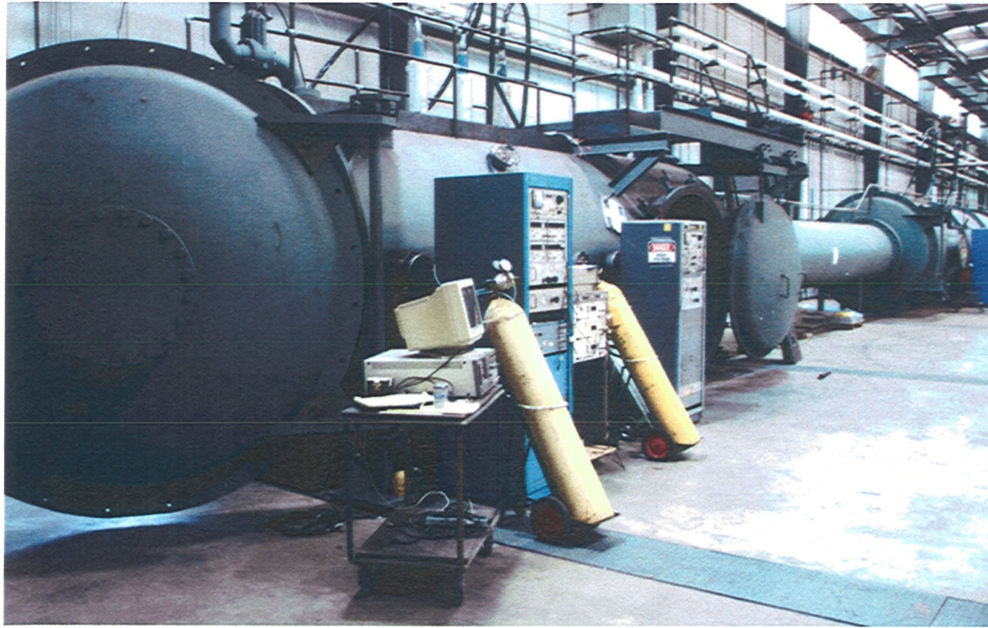


Figure 5.2 133 mm ARC LGG Impact Chamber

Table 5.1 133 mm LGG Dimensions

18.59 m Long x 133.35 mm" Diameter Pump Tube
15.24 m Long Interchangeable Launch Tubes
Launch Tube Diameters from 29.21 mm to 35.56 mm
3.05 m Long Blast Tank
2.44 m Diameter x 18.29 m Long Preflight Tank
9.15 m Long Optics Tank
2.44 m Diameter x 6.71 m Long Impact Chamber

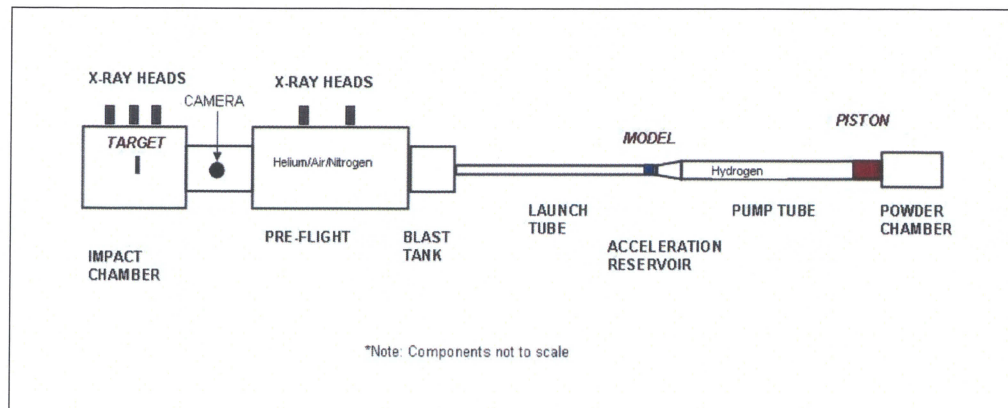


Figure 5.3 UAH ARC 133 mm LGG Range Schematic



The first stage of the gun consists of a powder charge driving a piston through hydrogen gas creating heat and pressure in the pump tube. This in turn opens a break valve allowing the hot gas to expand into the launch tube (second stage). The hot gas accelerates a sabot-mounted projectile to a maximum velocity. Once the projectile leaves the launch tube, the sabot separates and is stopped by the sabot catcher to prevent it from entering the impact chamber. X-ray film cassettes are placed along the flight path to capture the projectile pitch and yaw attitude. They are triggered when the projectile passes through a break screen interrupting a laser beam aligned with the shotline. Video can also be used to capture the projectile image just before impacting the target.

## *5.2 0744 Test Geometry*

Based on the predictions from PRODAS and RSM, the Run 2 projectile configuration produced the minimum predicted pitch and yaw attitude at impact. Therefore, this geometry was used to machine a projectile, numbered 0744, to launch in the 133 mm LGG. Figure 5.4 shows the final geometry of the 0744 projectile. The mid-body length (139.7 mm), cone angle ( $10^\circ$ ), and tail flare angle ( $50^\circ$ ) matched the specified geometry from Run 2. It was made up of the same materials as the original 0430 projectile. This included an aluminum rod with the same density change as the baseline to approximate a carbon steel rod with an epoxy sleeve. Due to miscommunication with the range, the 0744 projectile was modeled entirely of aluminum without a density change. Therefore, slight modifications were made to the body diameter and cone and tail length to closer match the predicted mass from the Run 2 PRODAS projectile. Table 5.2 shows the geometric differences. Figure 5.5 shows the

machined 0744 projectile. It was made from 6061-T6 aluminum and has a mass of 64.7 grams. It was 1.66 grams lighter than the PRODAS prediction of 66.36 grams even with the modifications. The RSM analysis was rerun with the actual aluminum density to verify that the error didn't substantially affect the results. The repeat runs showed a maximum difference of only  $0.07^\circ$  in pitch and  $0.04^\circ$  in yaw. The Run 2 configuration still predicted the minimum attitudes and was only  $0.01^\circ$  different from the original RSM predictions.

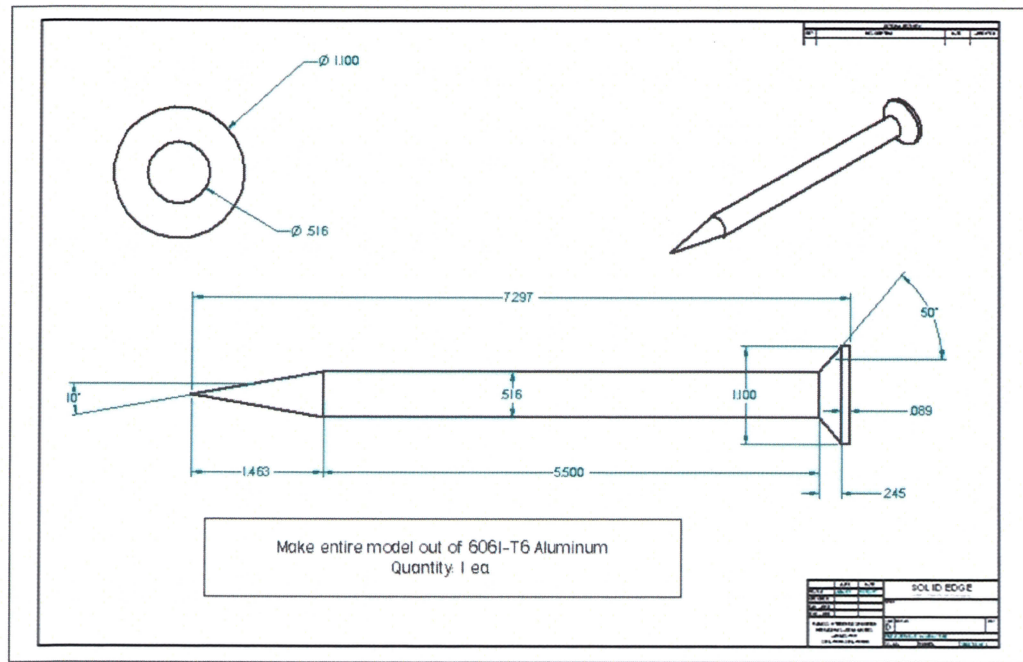


Figure 5.4 0744 ARC projectile (Dimensions in inches)

Table 5.2 Geometry Modifications

	Mid-Body Diameter (mm)/(in)	Cone Length (mm)/(in)	Tail Length (mm)/(in)	Total Length (mm)/(in)
Run 2	12.7/0.5	36.02/1.42	9.57/0.377	185.29/7.295
ARC 0744	13.106/0.516	37.16/1.46	8.48/0.334	185.34/7.297





Figure 5.5 0744 ARC Machined Projectile

### *5.3 0744 LGG Test and Results*

The final 0744 projectile was launched from the 133 mm LGG. The helium gas temperature was 295 K and the pressure was 726 torr (96.79 kPa). The average velocity for the test was 1507 m/s. These values were a little less than what was used for the predictions (300 K, 101.32 kPa, 1610m/s). The ARC likes to keep a negative pressure differential between the flight range and the ambient atmosphere (101.32 kPa/760 torr). This is to stop any potential leakage of the internal range gas which could include hydrogen. It also allows the range to open up the vent valves after the test and allow air into the gun. When the range gets close to ambient pressure, the air scrubber is turned on and a vent is opened into the range. The scrubber pulls in fresh air from the launcher end of the gun and sucks it out the other end. It is routed through filters to catch debris and then ejected into the atmosphere outside the building. This process puts breathable air back into the gun as well as taking the hydrogen out. Based on the pressure scaling from Section 3.3, the pressure was much higher than the original 0430 baseline test

(13.33 kPa/100 torr). The helium gas was therefore denser and caused the model to be slower.

The results of the 0744 test were well under the maximum requirement of  $2^\circ$  for pitch and yaw attitude upon impact. Figure 5.6 shows the break screen used to trigger the x-rays before and after the test. The hole made from the projectile was 27.94 mm in diameter. This was the exact diameter of the tail of the projectile. This gave a good indication that the projectile flew straight. Figures 5.7 and 5.8 show x-rays for pitch and yaw attitude just before impact. The pitch is approximately  $0.4^\circ$  and the yaw is approximately  $0.3^\circ$  with a  $\pm 0.3^\circ$  uncertainty. These values are compared to the Run 2 predictions of  $1.21^\circ$  and  $0.52^\circ$ , respectively. Figure 5.9 shows the impact point before and after the test. A piece of metal from previous tests was used, but one can clearly see the new hole made from the 0744 projectile. It was also fairly round indicating the projectile flew reasonably straight. The 0744 test was a success based on the data collected. The goal of impact attitude under the maximum  $2^\circ$  limit was attained.

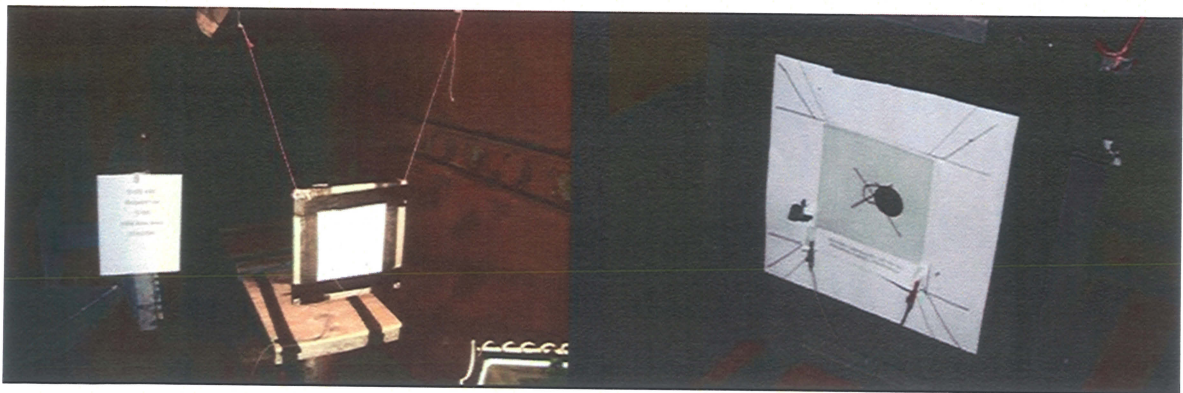


Figure 5.6 Break Screen Before and After 0744 LGG Test



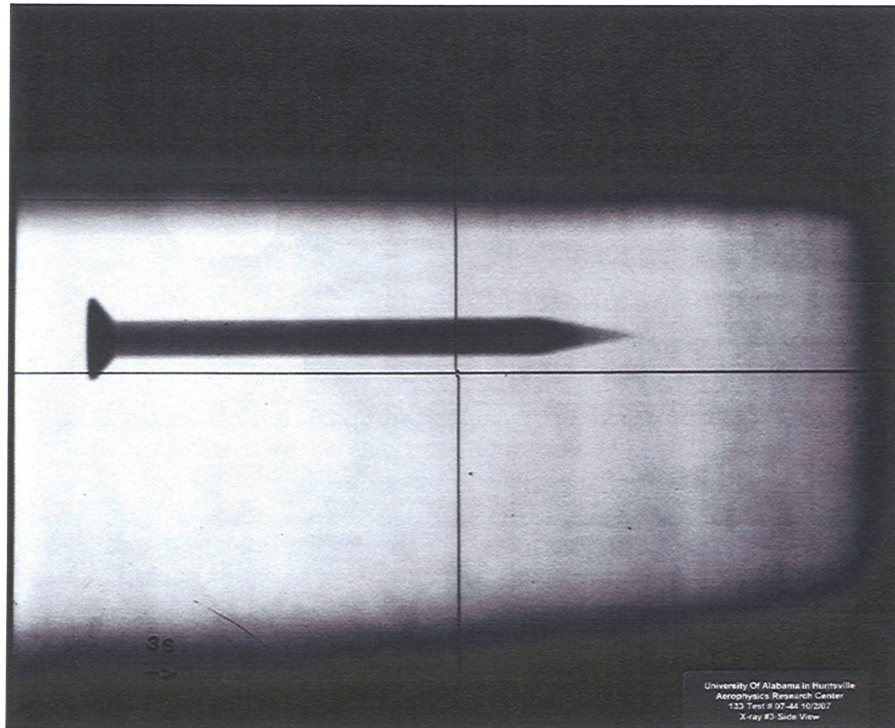


Figure 5.7 Pitch for ARC 0744 LGG Test

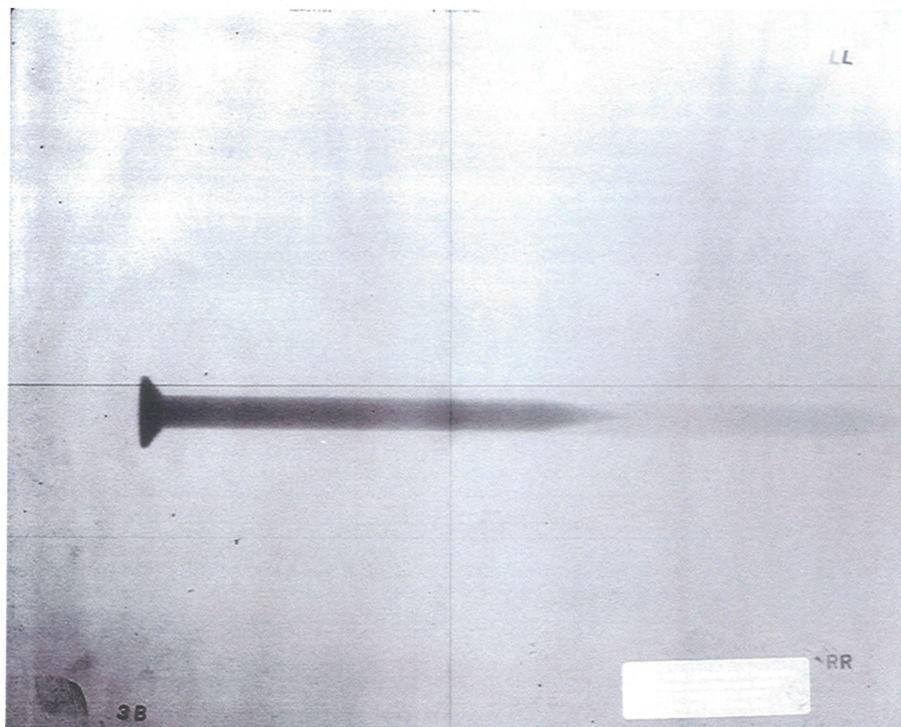


Figure 5.8 Yaw for ARC 0744 LGG Test

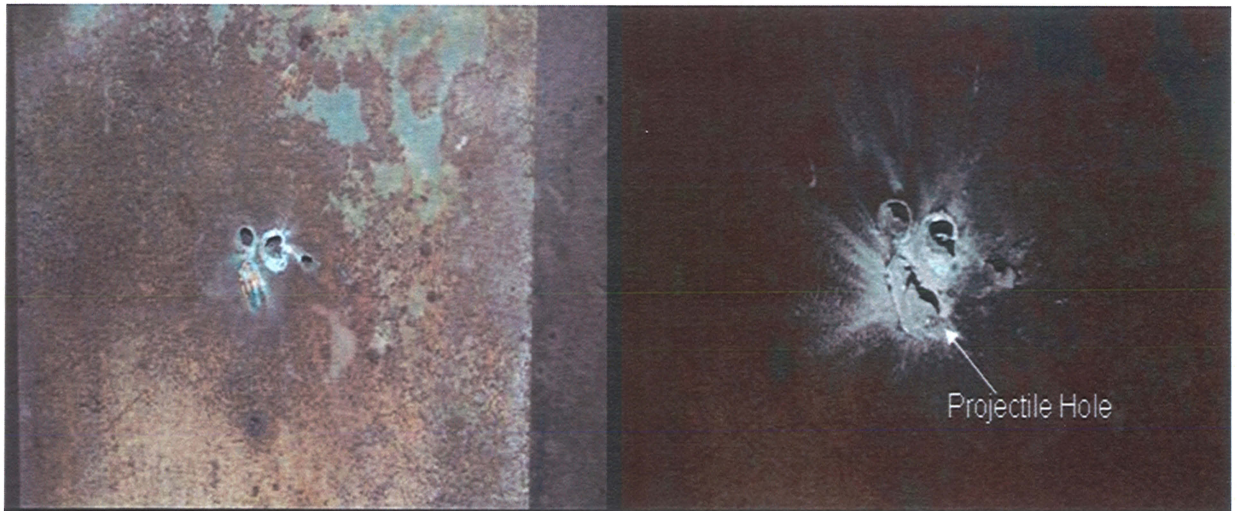


Figure 5.9 Impact Point Before and After 0744 LGG Test

#### 5.4 0744 PRODAS Model

PRODAS with pressure scaled air was used to predict the actual 0744 test.

Table 5.2 showed how the 0744 projectile geometry differed from the Run 2 configuration. The PRODAS *Aerodynamics* Model and *Stability Evaluation* screens for the 0744 projectile are shown in Figures 5.10 and 5.11. The projectile was modeled using 6061-T6 Aluminum just like the actual test with no density modifications as in the Run 2 configuration. This produced a mass of 64.98 grams that was within 0.28 grams of the actual 0744 projectile mass of 64.7 grams. The projectile CG was 112.903 mm from the nose.



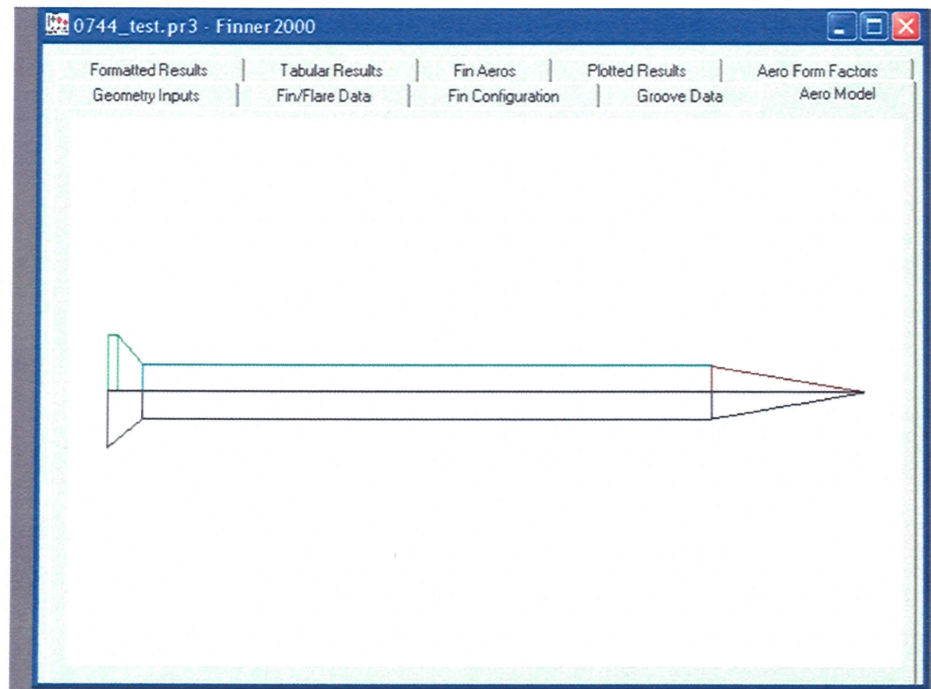


Figure 5.10 PRODAS Aerodynamics Model of 0744 Projectile [6]

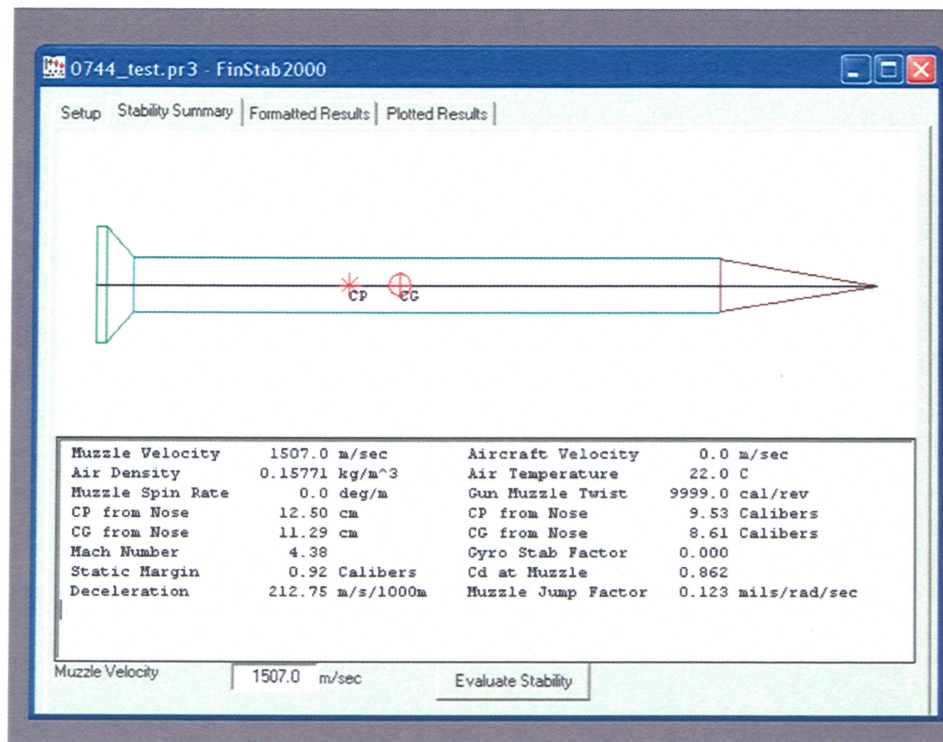


Figure 5.11 PRODAS Stability Evaluation Screen for 0744 Projectile [6]

### 5.5 0744 *PRODAS Trajectory Analysis*

Using a temperature of 295 K, a velocity of 1507 m/sec, baseline tip-off rates of 11.85 rad/sec for pitch and 5.05 rad/sec for yaw, and a pressure of 13.37 kPa, the *PRODAS Trajectory Analysis* was used to determine the pitch and yaw attitude. The pressure used was 7.237 times less than the actual test based on the scaling analysis (equation 3.10) from Chapter 3. The predicted pitch attitude was  $2.1^\circ$ , and the yaw was  $0.9^\circ$  as compared to the actual test of  $0.4^\circ$  and  $0.3^\circ$ , respectively. *PRODAS* over predicted the attitudes which is better than under predicting them. One unknown condition of the 0744 test was the actual tip-off rates. As discussed earlier, the range doesn't have the capability to measure tip-off rates, and they can vary from one test to the next. As was done for the baseline analysis, an iterative process was used to determine what the tip-off rates would need to be in order to match the 0744 test. Using the 0744 test day conditions and geometry, it was determined that a pitch tip-off of 2.25 rad/sec and a yaw tip-off of 1.7 rad/sec were need to match the  $0.4^\circ$  pitch and  $0.3^\circ$  yaw attitudes. Figures 5.12 and 5.13 show the pitch and yaw attitude for the *PRODAS* run using the baseline and modified tip-off rates. The attitudes are greatly reduced when less tip-off rate is present at launch.

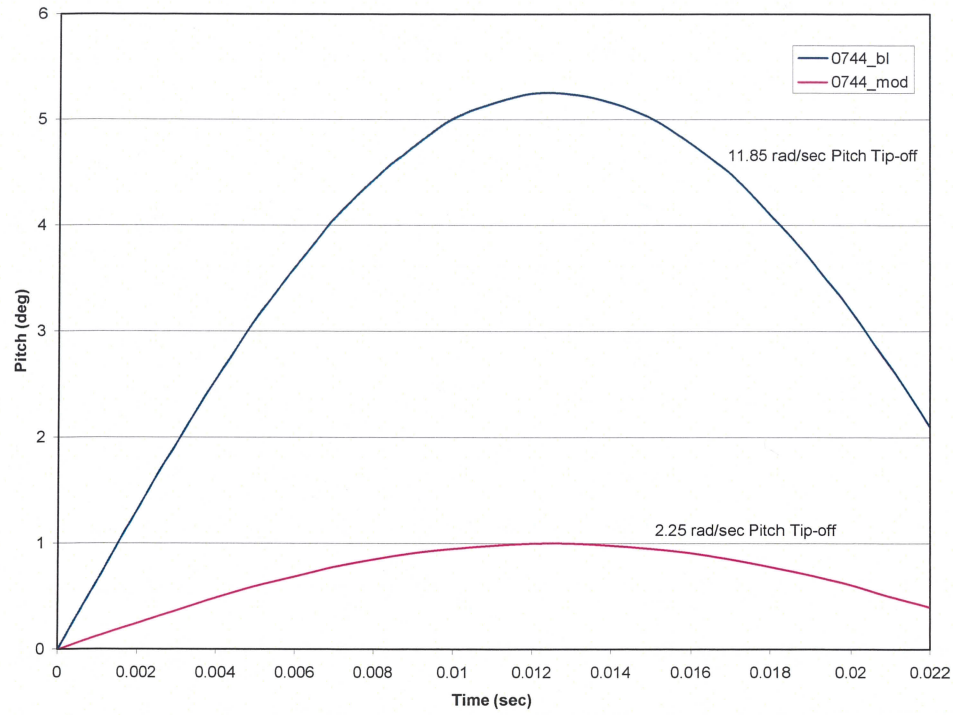


Figure 5.12 0744 PRODAS Predicted Pitch vs. Time for two Pitch Tip-off Rates

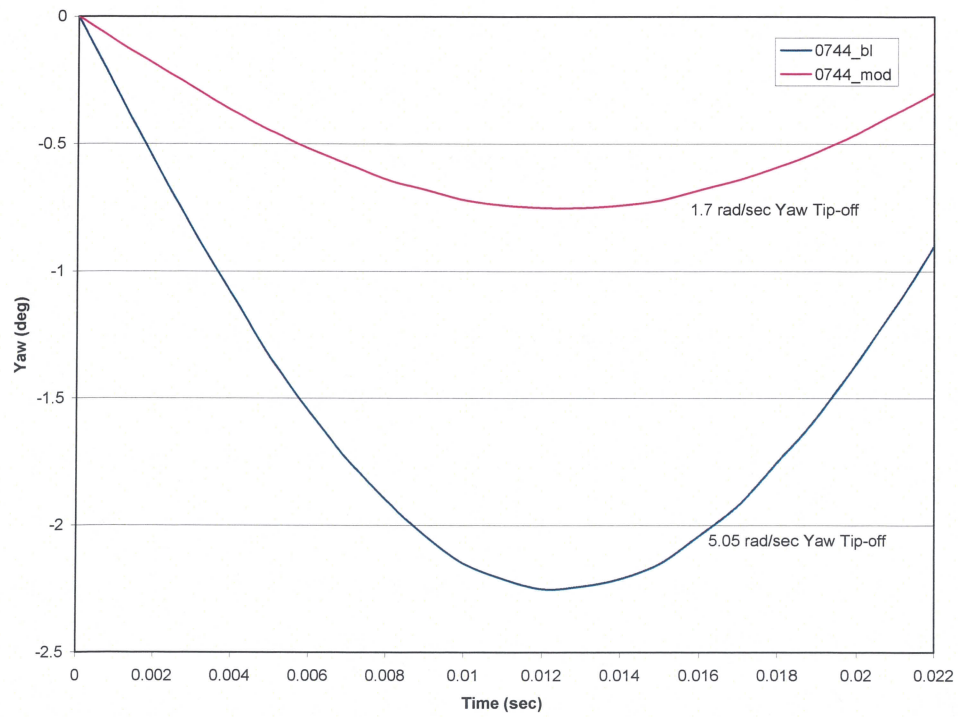


Figure 5.13 0744 PRODAS Predicted Yaw vs. Time for two Yaw Tip-off Rates

## **CHAPTER SIX**

### **SUMMARY AND CONCLUSIONS**

Hypervelocity impact testing is an important aspect of lethality assessment of tactical kinetic energy weapons. It was observed that light gas gun ballistic projectile tests in the University of Alabama in Huntsville Aerophysics Research Center (UAH ARC) produce unacceptably large impact angles ( $> 2^\circ$ ) in a helium test gas. However impact angles below this limit were consistently observed when nitrogen was used. A methodology was needed to design projectiles to meet impact angle requirements.

The Projectile Design and Analysis System (PRODAS) code provided a means to easily model a projectile geometry, determine its mass properties and stability, and predict its motion. However, PRODAS only simulates an air atmosphere. Various scaling methods were attempted based on traditional parameters of Mach, Froude and Reynolds number. After these attempts failed, a simple pressure scaling method was chosen. This method uses a modified ideal gas equation to calculate an equivalent air pressure with the density and temperature of the helium test gas.



An independent 6-DoF code, DigSim, was used to calibrate PRODAS and verify the pressure scaled air approach. A comparison of DigSim predictions of pitch and yaw attitude, velocity and downrange distance to PRODAS predictions in air provided a point of reference for the helium analysis. The results for the air analysis differed by no more than  $0.15^\circ$  for pitch and yaw attitude throughout the flight time. A DigSim model with a helium atmosphere and the 0430 baseline test parameters predicted the necessary tip-off rates (11.85 rad/sec pitch and 5.05 rad/sec yaw) to produce the measured pitch and yaw attitude upon impact. The modified ideal gas equation was used to calculate an equivalent scaled air pressure to run in PRODAS to simulate helium. PRODAS predictions using the scaled air pressure and estimated tip-off rates compared very well to the 0430 baseline test data and DigSim predictions. The pitch and distance were less than 1% different and the yaw was less than 4%. The attitudes were well within the  $\pm 0.3^\circ$  measurement accuracy given by the range.

Next, PRODAS was used to determine what pressure was needed to meet the  $2^\circ$  pitch and yaw attitude limit for the ARC. It was noticed that if the actual helium pressure of 13.33 kPa (from the 0430 LGG test) was used in the PRODAS simulation with air that the yaw attitude of  $1.04^\circ$  was well under the  $2^\circ$  limit, but the pitch attitude of  $2.43^\circ$  still exceeded it. Using equation 3.10 from Section 3.3, this would mean a range pressure of 96.47 kPa for the actual helium LGG test. When using a slightly higher pressure of 14 kPa (101.32 kPa for LGG), the predicted pitch was still over the  $2^\circ$  limit by  $0.09^\circ$  but well under the measurement accuracy ( $\pm 0.3^\circ$ ) given by the range.

The Response Surface Method (RSM) was next used with the PRODAS code and the 14 kPa pressure to efficiently analyze a matrix of projectile mid-body length, cone and tail angles. This matrix consisted of 15 PRODAS runs with different geometric configurations based on a high, nominal, and low characteristic. At least five configurations produced impact angles below the requirement. The configuration with the minimum pitch and yaw impact attitude was chosen for further study.

The new projectile configuration (0744) was fabricated and shot in the ARC ballistic range. At impact, a pitch attitude of  $0.4^\circ$  and yaw of  $0.3^\circ$  were measured versus the predictions from the Run 2 configuration of  $1.21^\circ$  and  $0.52^\circ$ , respectively. A final PRODAS run was made using the exact 0744 projectile geometry and test day conditions. It didn't have the approximated aluminum mid-body as did the Run 2 configuration. The same tip-off rates (11.85 rad/sec pitch and 5.05 rad/sec yaw) were used, but the final run had a lower velocity, pressure, and temperature (1507 m/sec, 13.37 kPa, 295 K) that corresponded to the actual test. At impact, a pitch attitude of  $2.1^\circ$  and yaw of  $0.9^\circ$  were measured versus the predictions of  $0.4^\circ$  and  $0.3^\circ$ , respectively. This difference was most likely due to the unknown value of the tip-off rates for the actual test. An iterative process was used to determine the tip-off rates (2.25 rad/sec for pitch and 1.7 rad/sec for yaw) needed to predict measured impact angles. This shows the high test-to-test variability of tip-off rates. Further analysis on multiple LGG tests is needed to better understand this variability.

Overall, this study showed that PRODAS with a scaled air can be used to reasonably predict projectile motion and thus aid projectile design. One drawback is that the air pressure predicted for the typical projectile geometries corresponds to a high actual helium test pressure at the limit of normal range operation. Another issue is the effect of the variable tip-off rates. But the significance of this is reduced by the fact that assuming high tip-off rates will over predict the impact angles. This will push the design toward a geometry that is even more within the impact attitude requirements. PRODAS is cost effective and provides the analyst a means to rapidly run a matrix of geometries and test conditions. RSM also provides an efficient method for using the PRODAS code to identify the geometric parameters that most affect meeting the test requirements. Further study of multiple LGG tests would provide assurance of the approach presented in this thesis.

## APPENDIX

### DigSim SAMPLE INPUT FILE

```
{ MLRS 6-DOF simulation nominal input data deck
{ SCCS ID: %W%
{
{ Date last delta applied: %G% %U%
{
{ Define glossary file
{
Glossary 'glossary.dat'
{
{ Simulation set-up
{
Set DtMax    = 0.0001
Set DtMin    = 0.0001
Set Time0    = 0.0
Set TStop    = 0.06
Set TPrint0  = 0.0
Set TPlot0   = 0.0
Set TOut0    = 0.0
Set DtOut    = 1.0
Set DtPrint  = 0.25
Set DtPlot   = 0.001
Set Eighty_Col = .False.
{-----
{ Set up Scenario
{
{ Set Launch Azimuth and Launch Elevation
{
Set Launch_Elevation_Angle_dg = 1.00000000e0
Set Launch_Az_True_North_dg  = 0.00000000e0
Set Lnch_Tgt_Az_dg           = 0.00000000e0
{
{ Input muzzle velocity in ft/sec
```



```

Set muzzle_velocity      = 5282.15e0
{
{ Set Timed Events
{
{ Set Launch and Impact Altitudes above Sea Level
{
Set Altg_r              = 0.00
Set Impact_Area_Altitude = 0.00
{
{ Set Launcher Position - LC33
{
Set Latg_r_dg           = 37.846009167e0
Set Long_r_dg           = -116.707808600e0
{
{ Set Mass Properties
{ wbo in lbs, xcg in ft, ixxbo, iyybo, izzbo in slug-ft^2
Set wbo                  = 0.1583
Set xcgbo                = 0.371063
Set ixxbo                = 1.5928e-6
Set iyybo                = 1.5489e-4
Set izzbo                = 1.5489e-4
{
Set Tip_Off_Duration    = 0.002
{P-roll Q-pitch R-yaw (rad/sec)
Set Q_br_b_IC          = 11.85
Set R_br_b_IC          = 5.05
Set P_br_b_IC          = 0.02
Set Atmos_Temp_C        = 27.0
Set Atmos_Press_Mb      = 133.32237
{
{ Input Gas constant in (ft lb)/(slug R)
{ Air    = 1718 gamma = 1.4
{ Helium = 12420 gamma = 1.67
{ Nitrogen = 1775 gamma = 1.4
{
Set Atmos_Gas_Const     = 12420.0
Set Atmos_Gas_gamma     = 1.67
{-----
{ Output
{
Plot Time
Plot X_br_r
Plot Y_br_r
Plot Altg_b_real
Plot Vel_bw
Plot Alpha_total_deg

```

```
Plot Alpha_deg
Plot Beta_deg
Plot Mach
Plot Q_br_b
Plot R_br_b
Plot Atmos_Density_slug_per_ft3
Plot Atmos_SoS
{
Run 1
Sto
```

## REFERENCES

- [1] “UAH/Aerophysics Research Center”, U.S. Army Space and Missile Defense Command, Huntsville, AL. [http://www.smdc.army.mil/FactSheets/UAH-ARC%20trifold%20info.pdf. Accessed 1/1/06.]
- [2] “PRODAS, A User’s Manual”, Arrow Tech Associates, South Burlington, VT, January 2004.
- [3] “PRODAS, A Technical Manual”, Arrow Tech Associates, South Burlington, VT, January 2004.
- [4] Brewer, V., “DigSim Driver v1.1, A User’s Guide”, Nichols Research Corporation, NRC-TR-90-128, Huntsville, AL, September 1992.
- [5] Myers, R., and Montgomery, D.C., *Response Surface Methodology: Process and Product Optimization Using Designed Experiments 2<sup>nd</sup> ed.*, John Wiley and Sons, New York, 2002.
- [6] PRODAS v3 Software Package, [www.prodas.com](http://www.prodas.com), Arrow Tech Associates, South Burlington, VT, January 2004.
- [7] Whyte, Robert H., "Spinner" – “A Computer Program for Predicting the Aerodynamic Coefficients of Spin Stabilized Projectiles”, General Electric Company, August 1969.
- [8] Nicolaidss, J. D., Eikenberry, R. S., Ingram, C. W., and Clare, T. A., "Flight Dynamics of the Basic Finner Missile", AFATL, Eglin Air Force Base, FL, Report No. TR-68-82, July 1968.
- [9] Kendric, G. W., and Gipson, B., “Earth v1.1 Module Report”, NRC-TR-95-038, Huntsville, AL, December 1994.
- [10] Blake, W. B., “Missile DATCOM, A Users Manual”, Air Force Research Laboratory, Wright Patterson Air Force Base, OH, 1998.
- [11] Schmidt, E. M., and Donovan, W. F., “Aerodynamic Control of Yaw and Jump of Fin-Stabilized Projectiles”, AIAA Paper 97-0424, January 1997.

- [12] Wolowicz, C. H., Bowman, J. S. Jr., and Gilbert, W. P., "Similitude Requirements and Scaling Relationships as Applied to Model Testing", NASA TP-1435, August 1979.